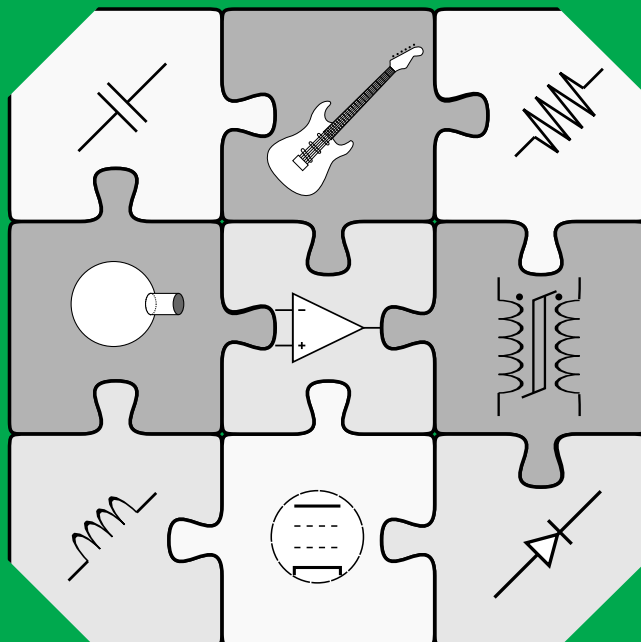


Circuit modeling studies related to guitars and audio processing

Rafael Cauduro Dias de Paiva



Circuit modeling studies related to guitars and audio processing

Rafael Cauduro Dias de Paiva

A doctoral dissertation completed for the degree of Doctor of Science (Technology) (Doctor of Philosophy) to be defended, with the permission of the Aalto University School of Electrical Engineering, at a public examination held at the lecture hall TU 2 of the school on 8 November 2013 at 12:00.

Aalto University
School of Electrical Engineering
Department of Signal Processing and Acoustics
Laboratory of Acoustics and Audio Signal Processing

Supervising professor

Vesa Välimäki

Thesis advisor

Jyri Pakarinen

Preliminary examiners

Prof. Dr. Augusto Sarti, Politecnico di Milano, Italy

Dr. Martin Holters, Helmut Schmidt University, Germany

Opponent

Dr. Thomas Hélie, IRCAM, France

Aalto University publication series

DOCTORAL DISSERTATIONS 167/2013

© Rafael Cauduro Dias de Paiva

ISBN 978-952-60-5387-5

ISBN 978-952-60-5388-2 (pdf)

ISSN-L 1799-4934

ISSN 1799-4934 (printed)

ISSN 1799-4942 (pdf)

<http://urn.fi/URN:ISBN:978-952-60-5388-2>

Unigrafia Oy

Helsinki 2013

Finland



Author

Rafael Cauduro Dias de Paiva

Name of the doctoral dissertation

Circuit modeling studies related to guitars and audio processing

Publisher School of Electrical Engineering**Unit** Department of Signal Processing and Acoustics**Series** Aalto University publication series DOCTORAL DISSERTATIONS 167/2013**Field of research** Audio signal processing**Manuscript submitted** 4 June 2013**Date of the defence** 8 November 2013**Permission to publish granted (date)** 25 September 2013**Language** English **Monograph** **Article dissertation (summary + original articles)****Abstract**

This thesis addresses the use of circuit modeling techniques in audio. Circuit modeling has a wide range of applications in audio, including real-time models of analog electronic audio equipment and the use of physical analogies for understanding and simulating musical instruments. Modeling of analog audio equipment is an important topic in audio signal processing. It enables the development of musical software that is capable of simulating rare vintage equipment at a low cost. This type of software can be embedded in portable electronic equipment, in mobile phones or tablets, or in computers.

This thesis presents novel models of analog audio equipment used with guitars. It presents a nonlinear audio-transformer model which is used for real-time emulation of vacuum-tube guitar amplifiers. This model has shown that some audio transformers have nonlinear effects for input signals with frequencies below 100 Hz. A new wave-digital model for operational amplifiers is proposed, which is used to simulate a wide class of guitar distortion circuits. The same distortion circuits were modeled with a novel method based on nonlinear system identification, which is enhanced using principal component analysis (PCA) for reduced complexity. It was shown that the proposed method reduces the complexity of the polynomial-Hammerstein model obtained with the swept-sine technique by 66 %. Additionally, electromagnetic pickups were analyzed and modeled, leading to new pickup-mixing and nonlinearity models and to a better understanding on the effects of guitar pickup and cable interaction.

This thesis has also presented how to use physical analogies for audio synthesis. Electro-acoustic analogies were used in order to obtain a model of connected Helmholtz resonators, resulting in the so called Helmholtz resonator tree. This model was implemented using wave-digital filters, which enables musical synthesis using physical descriptors that are intuitive also for non-technical users.

This thesis includes contributions for the application of circuit modeling techniques in audio. The audio transformer, electromagnetic pickup, and effect-box modeling developments are important for building real-time systems for audio effects and for preserving the heritage of vintage analog equipment. Finally, the electro-acoustic analogies presented show that circuit modeling can be used for abstract musical synthesis, where a virtual instrument can be excited in different manners yielding interesting timbre variations.

Keywords Nonlinear circuits, audio systems, real-time systems, circuit simulation, computer generated music

ISBN (printed) 978-952-60-5387-5**ISBN (pdf)** 978-952-60-5388-2**ISSN-L** 1799-4934**ISSN (printed)** 1799-4934**ISSN (pdf)** 1799-4942**Location of publisher** Helsinki**Location of printing** Helsinki**Year** 2013**Pages** 166**urn** <http://urn.fi/URN:ISBN:978-952-60-5388-2>

Preface

During the course of this work, I had the opportunity of being among really nice and competent people. It was a great pleasure to be a part of the Laboratory of Acoustics and Audio Signal Processing, where I have found a really pleasing and collaborative environment, which supports people on the great work they do.

This thesis was supported from CIMO and Nokia Foundation.

I would like to thank my supervisor, Professor Vesa Välimäki, who have done a great job in providing guidance and motivation. His vision on the whole picture of the signal processing field has helped me to value my ideas. Thanks also for my instructor, Jyri Pakarinen, for the support and the great technical discussions we had during the course of this work and all the help. Thanks for my coauthors Stefano D'Angelo, Miikka Tikander, and Henri Penttinen, for the technical discussions and their great contributions that enriched our publications. Thanks for Julian Parker and Luis de Jussilainen Costa, with whom I have improved substantially my English writing skills. Thanks for Sami Oksanen, who has been of great help in many procedures I had to do in the university.

I also extend my gratitude for the colleagues of the Laboratory of Acoustics and Audio Signal Processing: Antti Jylhä, Archontis Politis, Cumhuri Erkut, Giacomo Vairetti, Hannu Pulakka, Heidi-Maria Lehtonen, Heidi Koponen, Heikki Tuominen, Henna Tahvanainen, Javier Bolaños, Jussi Hynninen, Jussi Pekonen, Jussi Rämö, Leonardo Gabrielli, Luca Remaggi, Marko Hiipakka, Marko Takanen, Mikko-Ville Laitinen, Okko Räsänen, Olli Rummukainen, Olli Santala, Symeon Delikaris-Manias, Tapani Pihlajamäki, Teemu Koski, Tuomo Raitio, and Ville Pulkki.

Thanks for the pre-examiners Martin Holters and Augusto Sarti for the suggestions that helped to improve the quality of this work.

Thanks for Robson Vieira and David Gallegos, from INdT in Brazil, and

Mikko Säily, from Nokia Siemens Networks, who have helped me to keep on working while pursuing my doctoral studies.

Thanks for all the friends that I have made outside the university, and that were like a family during the time I have been in Finland: Cássio Ribeiro and family, Elizabeth and Maria Eduarda Vasconcelos, Ioannis Kotsionis, Irene Nousiainen, Juan Polanco and family, and Rodrigo Paiva.

Thanks for my parents, João Batista and Eloiza, for being such a great model of researchers which has inspired my career.

I would like to say special thanks for my wife, Juliana, who had embraced the challenge of moving to Finland, and have given me motivation and strength to conclude this work. Additionally, thanks for bringing the biggest joy of our lives, our daughter Helena.

Santa Maria, Brazil, October 15, 2013,

Rafael Cauduro Dias de Paiva

Contents

Preface	1
Contents	3
List of Publications	5
Author's Contribution	7
1. Introduction	15
2. Circuit modeling techniques	19
2.1 Physical models	19
2.2 Physically inspired methods	21
2.3 State space methods	21
2.3.1 The K method	22
2.3.2 Methods for obtaining the system equations	23
2.4 Wave digital filters	24
2.4.1 Wave digital filter networks	24
2.4.2 Linear elements	25
2.4.3 Nonlinear elements	27
2.4.4 Computational complexity	29
2.5 Black-box methods	29
2.5.1 Swept-sine methods	30
2.6 Discussion	33
3. Application of circuit modeling of the guitar	35
3.1 Effect box modeling	36
3.2 Guitar amplifier modeling	40
3.3 Guitar pickup	47
4. Circuit analogies for audio processing and synthesis	53

4.1	Physical analogies	53
4.2	Applications	55
5.	Summary of the main contributions	57
5.1	Publication I. Acoustics and modeling of pickups	57
5.2	Publication II. Cable matters: Instrument cables affect the frequency response of electric guitars	57
5.3	Publication III. Real-time audio transformer emulation for virtual tube amplifiers	59
5.4	Publication IV. Emulation of operational amplifiers and diodes in audio distortion circuits	60
5.5	Publication V. Reduced-Complexity Modeling of High-Order Nonlinear Audio Systems Using Swept-Sine and Principal Component Analysis	61
5.6	Publication VI. The Helmholtz resonator tree	61
6.	Conclusions and directions of future research	63
	Bibliography	67
	Errata	83
	Publications	85

List of Publications

This thesis consists of an overview and of the following publications which are referred to in the text by their Roman numerals.

I R. C. D. Paiva, J. Pakarinen, and V. Välimäki. Acoustics and modeling of pickups. *J. Audio Engineering Society*, vol. 60, no. 10, pp. 768–782, Oct. 2012.

II R. C. D. Paiva and H. Penttinen. Cable matters: Instrument cables affect the frequency response of electric guitars. In *Proc. 131st Audio Engineering Society Conv.*, New York, USA, paper number 8466, Oct. 2011.

III R. C. D. Paiva, J. Pakarinen, V. Välimäki, and M. Tikander. Real-time audio transformer emulation for virtual tube amplifiers. *EURASIP J. Advances Signal Processing*, pp. 1–15, Feb. 2011.

IV R. C. D. Paiva, S. D’Angelo, J. Pakarinen, and V. Välimäki. Emulation of operational amplifiers and diodes in audio distortion circuits. *IEEE Trans. Circuits and Systems - Part II, Express Briefs*, vol. 59, no. 10, pp. 688–692, Oct. 2012.

V R. C. D. Paiva, J. Pakarinen, and V. Välimäki. Reduced-complexity modeling of high-order nonlinear audio systems using swept-sine and principal component analysis. In *Proc. AES 45th Conf. Applications of Time-Frequency Processing in Audio*, Espoo, Finland, pp. 1–4, Mar. 2012.

- VI** R. C. D. Paiva and V. Välimäki. The Helmholtz resonator tree. In *Proc. DAFx'12, 15th Int. Conf. Digital Audio Effects*, York, UK, pp. 413–420, Sep. 2012.

Author's Contribution

Publication I: “Acoustics and modeling of pickups”

The author planned this study in collaboration with the co-authors. The author of this thesis developed the models, performed the simulations, reviewed the bibliography on the topic, and was the main writer of the paper except for the abstract.

Publication II: “Cable matters: Instrument cables affect the frequency response of electric guitars”

The author and the co-author planned this study. The author derived the cable model, wrote the paper, and designed, performed, and analyzed the cable measurements.

Publication III: “Real-time audio transformer emulation for virtual tube amplifiers”

The author of this thesis designed the measurement setup and the model parameter fitting procedure, wrote the paper (except for the abstract and Section III), and developed, implemented, and validated the proposed model.

Publication IV: “Emulation of operational amplifiers and diodes in audio distortion circuits”

The author derived the operational amplifier model, defined the Lambert function approximation method using a look-up table for the initial value,

implemented the models and verified them using Matlab, and evaluated the computational cost. Stefano D'Angelo derived the diode model using the Lambert function. The author also wrote the paper, except for Section III.

Publication V: “Reduced-complexity modeling of high-order nonlinear audio systems using swept-sine and principal component analysis”

The author planned this study in collaboration with the co-authors. The author extended the swept-sine method using PCA, implemented and tested the method in Matlab, and was the main writer of the paper.

Publication VI: “The Helmholtz resonator tree”

The author derived the model, implemented the method, and analyzed it. The author wrote the paper except for the abstract.

List of Abbreviations

DWG	Digital waveguide
FEM	Finite element method
FIR	Finite impulse response
FTM	Functional transformation method
ODE	Ordinary differential equation
PCA	Principal component analysis
PDE	Partial differential equation
MNA	Modified nodal analysis
MIMO	Multiple-input multiple-output
RLC	Resistor, inductor, and capacitor circuit
SS	State-space circuit (simulation method)
WDF	Wave-digital-filter circuit (simulation method)

List of Symbols

A	WDF incoming wave
\mathbf{A}	SS matrix for mapping the states vector onto the states derivative
\mathbf{A}_k	WDF k^{th} adaptor
B	WDF outgoing wave
\mathbf{B}	SS matrix for mapping the input vector onto the states derivative
c	Speed of sound in the air
C	Electrical capacitance, or acoustical capacitance of a cavity
\mathbf{C}	SS matrix for mapping the nonlinear function outputs onto the states derivative
d	Mechanical damping factor
\mathbf{D}	SS matrix for mapping the states vector onto the nonlinear mapping function input
E	Electrical voltage source
\mathbf{E}	SS matrix for mapping the input vector onto the nonlinear mapping function input
$\mathbf{f}(\cdot)$	SS nonlinear mapping function
f_i	Swept-sine initial frequency
$f_e(\cdot)$	Nonlinear voltage/current mapping function
$f_i(t)$	Swept-sine input signal
f_s	Sampling frequency
$f_W(\cdot)$	WDF Nonlinear mapping function in the wave domain
F	Mechanical force
\mathbf{F}	SS matrix for mapping the input vector onto the nonlinear mapping function input
$\mathbf{g}(\cdot)$	K-method inverse mapping for SS models
G_{inv}	Operational amplifier inverting configuration gain
G_{noninv}	Operational amplifier inverting configuration gain
H	Pickup magnetizing force
\mathbf{H}	Discrete-time SS state vector mapping function

\mathbf{i}	SS nonlinear mapping function output vector
I	Electrical current
I_p	Amplifier plate current
k	Mechanical spring constant
\mathbf{K}	K-method matrix solution for SS models
l	Length of a tube
L	Electrical inductance, or acoustical inductance of a tube
\mathbf{L}	SS matrix for mapping the states vector onto the output vector
\mathbf{L}_k	WDF k^{th} leaf element
m	Mechanical mass
\mathbf{M}	SS matrix for mapping the input vector onto the output vector
\mathbf{N}	SS matrix for mapping the nonlinear function outputs onto the output vector
p	Acoustical pressure
\mathbf{p}_n	n^{th} sample of the discrete-time SS nonlinear solution input vector
R	Electrical resistance, or acoustical fluid-dynamic resistance
R_{NL}	Nonlinear resistance
R_s	Amplifier series resistance
R_p	WDF port resistance
\mathbf{R}	WDF root element
S	Cross-sectional area of a tube
t	Time variable
T_R	Swept-sine exponential increase rate
v	Mechanical velocity
\mathbf{v}	SS nonlinear mapping function input vector
\mathbf{v}_n	n^{th} sample of the discrete-time SS nonlinear mapping function input vector
V	Electrical voltage, or volume of a cavity
V_{cc}	Amplifier power source
V_{gk}	Amplifier gate-to-cathode voltage
V_{i0}, V_{i1}	Operational amplifier input voltages
V_{in}	Amplifier input voltage
V_{pk}	Amplifier plate-to-cathode voltage
V_{out}	Operational amplifier output voltage
u	Mechanical volume flow
\mathbf{u}	SS input vector
\mathbf{u}_n	n^{th} sample of the discrete-time SS input vector

\mathbf{x}	SS state vector
\mathbf{x}_n	n^{th} sample of the discrete-time SS state vector
\mathbf{y}	SS output vector
\mathbf{y}_n	n^{th} sample of the discrete-time SS output vector
Z_0, Z_1	Operational amplifier input impedances
Z_f	Operational amplifier feedback impedance
α	SS discretization coefficient
δt_m	Swept-sine time shift for the m^{th} harmonic
μ	Pickup magnetic permeance
ρ	Air density
ϕ	Pickup magnetic flux

1. Introduction

Circuit modeling has important applications for audio signal processing which range from digital audio effects processing that are designed based on models of real-world devices to new musical instruments that are built based on physically inspired blocks.

Recent research activity has been devoted to building digital models of analog systems, or *Virtual analog* systems [1, 2, 3]. This field of research focuses on obtaining models of vintage audio equipment used for musical synthesis or effects. An application of this field is to substitute bulky and expensive analog equipment with software. Figure 1.1 shows an example of electronic components required for building a single guitar amplifier. When virtual analog techniques are used, all the components of Fig. 1.1 can be modeled in a software, and a computer, a portable electronic device, a mobile phone or tablet could accommodate several amplifier models.

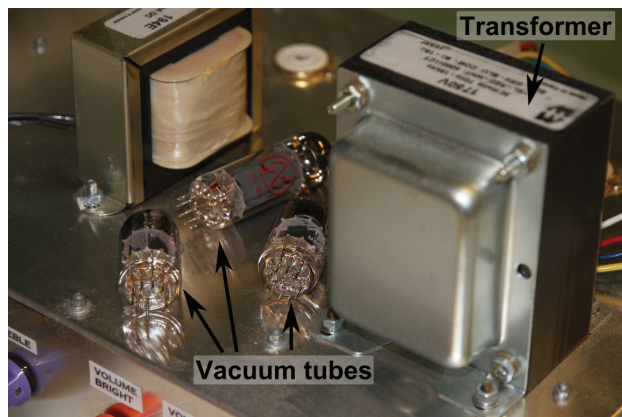


Figure 1.1. Example of components required for building a guitar amplifier, including vacuum tube devices and electric transformers.

Obtaining models of vacuum-tube amplifiers and guitar distortion effects has been an important focus of virtual analog studies. Although vacuum-tube devices have been replaced almost entirely in the industry

by solid-state devices, they are still appreciated in audio equipment, particularly in electric guitar applications. However, since vacuum tube components have now very strict commercial niches, their price is high when compared to solid state components [4]. For this reason, several publications have proposed models to emulate vacuum-tube devices using digital signal processing techniques [5]. Virtual analog models also include simulation of vintage analog synthesizers. For this purpose oscillator models [6, 7, 8, 9] and models of its nonlinear filters [10, 11, 12, 13, 14, 15] have been developed. Additionally, other analog electronic instruments such as the Clavinet have been modeled using virtual analog techniques [16, 17, 18]. Other applications of virtual analog include models of the diode ring modulator [19, 20], analog delay-line circuit [21], and spring reverberation [22, 23]. Several patents on vacuum tube amplifier models demonstrate the commercial importance of this kind of work [24, 25, 26, 27], and automatic amplifier modeling is also applied to commercial products [28].

Another focus of circuit modeling in audio is on the development of abstract musical synthesis, where users connect block-based physical models in physically meaningful ways [29], but which could also result in non-physically-realizable virtual systems. This means that by using physical analogies, users can intuitively change the parameters of virtual instruments. Several block-based techniques that can be used for synthesis are available in the literature [30, 31, 32].

The objectives of this dissertation are the following:

1. obtain new models of analog audio systems,
2. develop methods for real-time simulation of audio circuits,
3. develop black-box models of analog audio systems suitable for real-time implementation,
4. use circuit analogies for audio processing, and
5. use circuits physics to understand electroacoustic phenomena.

In Publications I, III, IV, and V analog models are built, which are in line with the objective 1. Objective 2 is addressed by Publications III and VI, in which real-time systems are developed, and in IV and V, where low-

cost models are developed for enabling real-time processing. The method described in Publication V is related to objective 3, since it enables significant complexity reduction of traditional audio black-box models. Publication VI is related to objective 4, and is deals with acoustic/electrical analogies, which are used for synthesis. Objective 5 is addressed by publications I, II, and III, since they can be used as tools for audio engineers and they provide an explanation for the behavior of guitar equipment.

This thesis is organized as follows. Section 2 presents some of the main methods for audio circuit simulation and includes a comparative discussion of the methods. The methods described in Section 2 are applied to the electric guitar in Section 3, where models for guitar effect-boxes, amplifiers, and pickup are also presented. Section 4 presents the use of physical analogies for musical synthesis, effects, and analysis of musical instruments. The contributions developed in this thesis are presented in Section 5. Section 6 concludes this thesis presenting final remarks and future research directions.

2. Circuit modeling techniques

Circuit models are mainly obtained with physical models and black-box techniques. Figure 2.1 shows a schematic overview of the difference between these techniques. Gray-box approaches, in which some insight of the structure of the circuit is included, are also available [5, 33]. The physical models are the ones in which the knowledge of the system and its internal states is used to build a model, whereas the black-box models only try to emulate the input/output relationship without considering the internal states of the system. The physical models include physically inspired methods, state space methods, as well as wave-digital filters. The black-box models discussed in this thesis include Volterra nonlinear filters, and swept-sine methods. This section presents the main techniques used for circuit modeling in audio, including physical models presented in Section 2.1 and black-box models presented in Section 2.5.

2.1 Physical models

Physical models comprise an important set of techniques used for audio circuit modeling. They have some advantages over other types of approaches, since they can flexibly change the circuit parameters, and they do not require measurements for building the model when information about the modeled components is available. These models are also able to emulate the behavior of physical systems under conditions which would not be realizable in reality. One example would be to simulate a circuit in which a real component is damaged because of extreme heating.

Physical models are obtained by inspection and calculation of the system equations, or by connecting blocks modeling the system's elements. The most traditional approach for physical modeling is to derive ordinary differential equations (ODE) for the system, discretize the equations

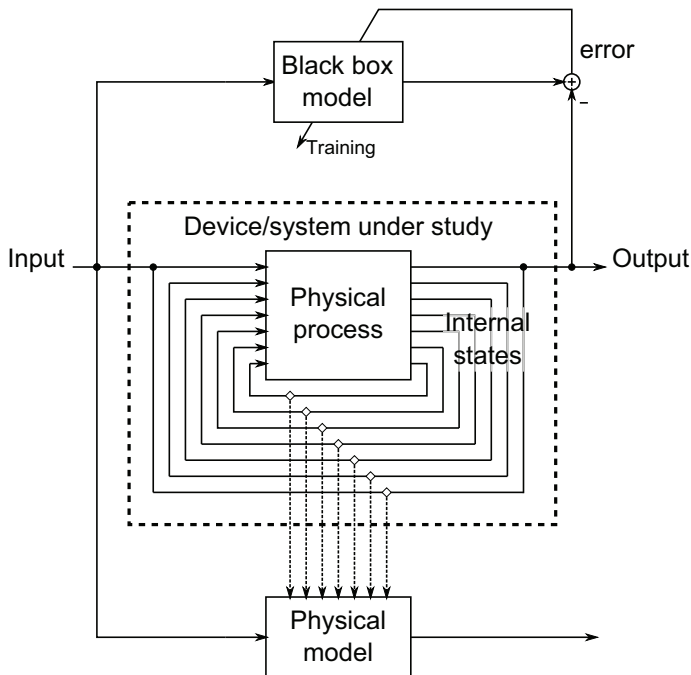


Figure 2.1. Overview of the difference between physical and black-box models.

using forward/backward Euler methods or the trapezoidal rule, and obtain the numerical solution of the implicit discrete nonlinear equations using a method such as Newton [34, 35, 19]. On the other hand, it is also possible to use the ODEs to derive filter structures that represent the equations [11]. Additionally, the frequency-dependent gain of linear systems can be discretized and applied as linear filters using a bilinear transform [36, 37]. One extension of the ODE-solving method is provided by state-space (SS) methods, which augment this concept by representing several system equations in a matrix form and provide systematic methods to obtain the system equations, as discussed in Section 2.3. Another approach is to use wave-digital-filters (WDF) to represent the system. When using WDFs, the physical variables are converted into wave-variables and the system is represented by traveling waves. This has the advantage of providing a block-wise representation of circuits and having linear computational complexity $\mathcal{O}(N)$ as a function of the number of circuit components. WDFs are discussed in Section 2.4.

2.2 Physically inspired methods

Physically inspired models comprise an important class of audio circuit modeling techniques. In this type of technique, the system designer attempts to understand the behavior of the system and designs a set of filters and waveshapers that emulate that behavior. Examples of the use of this technique include the models of the Moog filter [11, 6], a guitar distortion circuit [38], a sampler [39], a carbon microphone [40], and a diode ring-modulator [20]. This type of model is interesting for its simplicity and easy of application. However, the derivation of the model involves a time-consuming analysis of the system. Additionally, the final model may not be as accurate as one obtained with other techniques [38, 35], but it may capture the characteristic behavior of the system, such as the type of distortion.

2.3 State space methods

Most of the circuit modeling techniques are derived in matrix form representing the states of a system. This is a compact way of representing all the differential equations required to model the system behavior. The continuous-time representation of this type of system is given as [41, 42]

$$\dot{\mathbf{x}} = \mathbf{Ax} + \mathbf{Bu} + \mathbf{Ci}, \quad (2.1)$$

$$\mathbf{i} = \mathbf{f}(\mathbf{v}), \quad (2.2)$$

$$\mathbf{v} = \mathbf{Dx} + \mathbf{Eu} + \mathbf{Fi}, \quad (2.3)$$

$$\mathbf{y} = \mathbf{Lx} + \mathbf{Mu} + \mathbf{Ni}, \quad (2.4)$$

where \mathbf{x} is the state vector of the system, \mathbf{y} is the output vector of the system, \mathbf{u} represents the inputs, \mathbf{i} includes the nonlinear effects in the dynamics of the system, \mathbf{v} is the input vector for the nonlinear function, $\dot{\mathbf{x}}$ is the time derivative of \mathbf{x} , $\mathbf{f}(\mathbf{v})$ is a multiple-input multiple-output (MIMO) nonlinear mapping, and \mathbf{A} to \mathbf{F} and \mathbf{L} to \mathbf{N} are the matrices mapping \mathbf{x} , \mathbf{u} and \mathbf{i} to the states and the output. In order to simulate this system,

Eq. 2.1–2.4 can be discretized and rewritten as [41, 42]

$$\mathbf{x}_n = f_s \mathbf{H} \mathbf{x}_{n-1} + \mathbf{H} (\mathbf{B} \mathbf{u}_n + \mathbf{C} \mathbf{i}_n), \quad (2.5)$$

$$\mathbf{i}_n = \mathbf{f}(\mathbf{v}_n), \quad (2.6)$$

$$\mathbf{v}_n = \mathbf{D} \mathbf{x}_n + \mathbf{E} \mathbf{u}_n + \mathbf{F} \mathbf{i}_n, \quad (2.7)$$

$$\mathbf{y}_n = \mathbf{L} \mathbf{x}_n + \mathbf{M} \mathbf{u}_n + \mathbf{N} \mathbf{i}_n, \quad (2.8)$$

$$\mathbf{H} = (f_s \mathbf{I} + \mathbf{A})^{-1}, \alpha = f_s, \quad (2.9)$$

where f_s is the sampling frequency, \mathbf{H} is the discrete state update matrix, and \mathbf{I} is the identity matrix. Many techniques for discretization can be used, such as the forward/backward Euler methods or the trapezoidal rule [34, 35, 19], and it has been verified that the discretization method as well as the sampling frequency at which the circuit is calculated are directly related to the stability of the system [35].

The nonlinear system described above cannot be explicitly solved, since Eq. 2.6 involves the implicit dependence on \mathbf{i}_n . Traditional solutions to this problem involve an iterative solving process such as the Newton method [35, 43]. However, iterative solutions are typically avoided in real-time audio systems, since they are usually computationally expensive.

2.3.1 The K method

The K method proposes a solution for SS systems, which can be implemented in real-time without an iterative algorithm. In order to deal with this problem, it is possible to solve the nonlinear function [41]

$$\mathbf{0} = \mathbf{f}(\mathbf{p}_n + \mathbf{K} \mathbf{i}_n) - \mathbf{i}_n, \quad (2.10)$$

where

$$\mathbf{p}_n = \alpha \mathbf{D} \mathbf{H} \mathbf{x}_{n-1} + (\mathbf{D} \mathbf{H} \mathbf{B} + \mathbf{E}) \mathbf{u}_n \quad (2.11)$$

is the contribution of previously computed terms, and

$$\mathbf{K} = \mathbf{D} \mathbf{H} \mathbf{C} + \mathbf{F} \quad (2.12)$$

is the matrix for the delay-free path mapping the nonlinear function outputs and outputs. The solution of Eq. 2.10 is the nonlinear mapping

$$\mathbf{i}_n = \mathbf{g}(\mathbf{p}_n), \quad (2.13)$$

which can be either calculated online using iterative algorithms or computed offline and stored as a look-up table. Any change in the system parameters made by the user requires that the look-up table is recalculated

and updated. Once this mapping is found, the system can be evaluated online by using Eqs. 2.11, 2.13, 2.5, and finally Eq. 2.8 [41, 42]. Some variations on this algorithm are available, such as solving the nonlinear mapping as a function of \mathbf{v}_n instead of \mathbf{i}_n , which is claimed to converge faster [42].

The computational complexity of the K method is given by the matrix multiplications of Eq. 2.11, Eq. 2.13, Eq. 2.5, and Eq. 2.8 [44]. If asymptotic notation is used, this complexity can be approximated as $\mathcal{O}(N^2)$, where N is the number of states of the system.

2.3.2 Methods for obtaining the system equations

The SS system equations may be obtained by several ways. A possible solution is to derive the circuit differential equations and express them in the SS format of Eq. 2.1–2.4. Some examples of this approach are presented in [45, 46, 47, 48]. This approach has the advantage of having as many states as the number of capacitors and inductors, which often yields small matrices. However, deriving the system equations is a laborious task, and automatic methods for determining the model parameters are highly desirable.

The modified nodal analysis (MNA) is a traditional method used in circuit simulation. In this method, the Kirchoff equations of each node and a matrix template are used to build the model in a systematic manner [42]. Hence, this method has the great advantage of being scalable for building models of generic circuits. However, this type of technique results in large matrix representations, since all the nodes of the circuit need to be represented by Kirchoff's current law [49].

Generally, SS techniques can be applied efficiently when using the K method. However, a major problem is encountered in circuits with time-varying parameters, since the matrices of the SS model need to be updated every time one parameter is changed. In guitar circuits, users have access to potentiometers to modify the circuit parameters, hence modification of resistances in real-time is highly desirable when building these models. This problem can be addressed by decomposing the system matrices into smaller matrices that can enable faster update of the system once its parameters are changed [50].

2.4 Wave digital filters

Wave digital filters (WDF) comprise an efficient modular way of simulating circuits [30, 51, 32, 2]. This technique uses wave counterparts of electrical quantities in order to describe the circuit, which are given by [30, 52]

$$V = \frac{A + B}{2}, \quad (2.14)$$

$$I = \frac{A - B}{2R_p}, \quad (2.15)$$

$$A = V + R_p I, \quad (2.16)$$

$$B = V - R_p I, \quad (2.17)$$

where V and I are the electrical voltage and current, A and B are incoming and outgoing waves of an element, and R_p is the port resistance of this element. Other representations for Eq. 2.14–2.17 exist, an example being the equations modified for power normalization [51]. Notice that R_p is related to the WDF implementation and is not a physical resistance. In WDF networks, every circuit element is represented by a block, which is connected to the network by a port having port resistance R_p . These elements are interconnected to others by adaptors, which model the type of connection each element has. These include series or parallel connections, transformers, mutators [53, 54], gyrators [30, 52], and polarity-change adaptors [55]. The expressions for the outgoing waves of series and parallel connections are presented in Eqs. 7 and 8 of Publication III.

2.4.1 Wave digital filter networks

Figure 2.2 shows an example of a generic WDF network. In this example, circuit elements \mathbf{L}_k and \mathbf{R} are interconnected through adaptors \mathbf{A}_k . The network of Fig. 2.2 has one root element \mathbf{R} , K leaves \mathbf{L}_k , and $K - 1$ three-port adaptors \mathbf{A}_k . Figure 2.2 shows that the adaptors may have several ports, with each port having the same impedance as the impedance of the element it is connected to. This structure is called the binary connection tree (BCT) [56, 57]. Although most electrical circuits can be represented by a BCT, some may require other types of multiport connections in order to yield a computable WDF network, such as circuits with a Jaumann structure [58, 57].

WDF networks are connected in the tree-like structure of Fig. 2.2, where \mathbf{R} is the root and \mathbf{L}_k are the leaves of the tree. Additionally, the outgoing arrows of some elements are marked with a 'T' termination, which

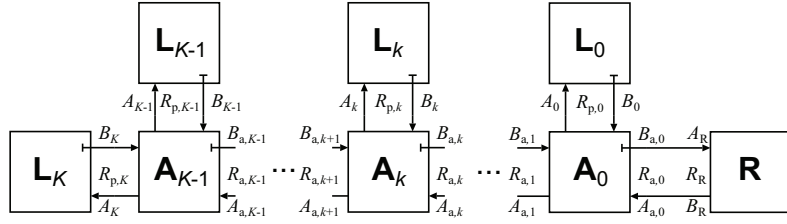


Figure 2.2. Generic WDF network. In this example, leaf elements are represented by \mathbf{L}_k , adaptors are represented by \mathbf{A}_k , and the root is represented by \mathbf{R} .

indicates that they are reflection-free ports. The reflection-free port notation is used when the outgoing wave of an element has no instantaneous dependency on its incoming wave, and circuit elements having reflection-free ports are called *adapted*. Notice that all the leaves have reflection-free ports, whereas the root does not. Moreover, all the reflection-free ports of the adaptors point in the direction in which the root is placed, and all the three-port adaptors in the literature can have a maximum of one reflection-free port.

The positioning of reflection-free ports is directly related to how the computation of WDF networks is performed. Figure 2.3 shows the calculation steps required for the type of network in Fig. 2.2 [56, 57]. In the first step, the leaves \mathbf{L}_k determine their outgoing waves B_k , based on the past values of their incoming waves A_k . In the second step, the adaptors \mathbf{A}_k use the information of the waves received by the leaves to determine their outgoing waves $B_{a,k}$ until they reach the root $B_{a,0}$. In the third step, the root is able to determine its outgoing wave B_R from the information of the incoming wave A_R . In the fourth step, the adaptors propagate the root outgoing wave until they reach the leaves \mathbf{A}_k . After this step, the voltages and currents of all physical elements can be computed using Eqs. 2.14 and 2.15. A C++ implementation of a WDF network based on this approach is included in Publication VI.

2.4.2 Linear elements

The expressions representing some linear circuit elements is shown in Table 2.1. This table shows two expressions for the outgoing wave. In the first, a generic expression is presented where the output depends on the input, whereas in the second the output is independent of the input [59]. The second expression enables the implementation of adapted elements with delay-free ports. Additionally, the condition for adaptation depends

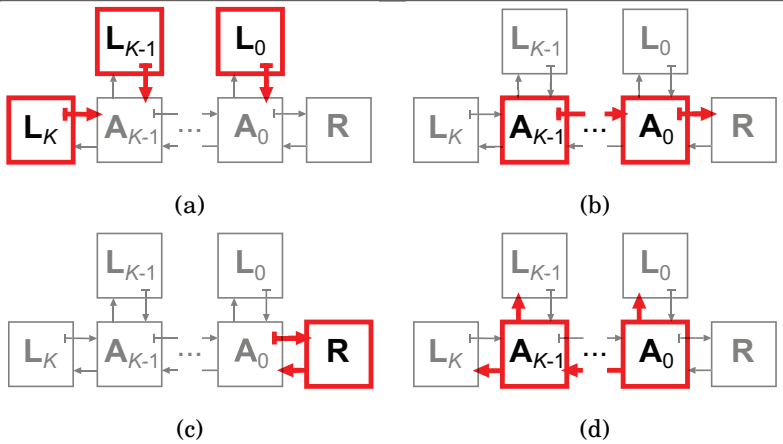


Figure 2.3. Calculation steps for each time sample of the generic network in Fig. 2.2. (a) Leaves calculate the output waves; (b) adaptors use incoming waves from leaves to calculate their output, propagating the waves until the root element is reached; (c) the root element calculates its output; and (d) the wave is propagated back to the leaves.

on the port resistance and is also described in Table 2.1 [30, 52]. Furthermore, Table 2.1 shows that building an ideal voltage source is impossible, since the outgoing wave cannot be determined if $R = R_p = 0$. However, this problem can be overcome by using a series or parallel adaptor combined with a voltage or current source [59].

Table 2.1. Description of some WDF elements with their adaptation condition, where R , C , f_s , E and R_p represent resistance, capacitance, sampling frequency, internal voltage, and the port resistance, respectively, and $\rho_c = 2f_s C$.

Element	Resistor	Capacitor	Voltage source with resistance
Output wave B	$B = A \frac{R-R_p}{R+R_p}$	$B = A \frac{1-\rho_c+(1+\rho_c)z^{-1}}{1+\rho_c+(1-\rho_c)z^{-1}}$	$B = \frac{2R_p E - A(R-R_p)}{R+R_p}$
Adaptation condition	$R_p = R$	$R_p = \frac{1}{\rho_c}$	$R_p = R$
Adapted output	$B = 0$	$B = Az^{-1}$	$B = E$

The same type of adaptation conditions described in Table 2.1 are described for the reflection-free port of adaptors [30, 52]. The series and parallel adaptors can have only one reflection-free port, and the impedance value of this port depends on the impedance of its other ports. As a result of the port impedance restrictions, if the impedance of an element is changed, the port impedances of the other WDF elements have to be changed accordingly. Figure 2.4 shows an example where an element L_k of a WDF network is changed. When this happens, the reflection-free port

impedance of all the adaptors in the path between the element \mathbf{L}_k and the root element \mathbf{R} have to be changed [56], otherwise instantaneous dependency will be added to the network, making computation scheduling impossible without iterative methods.

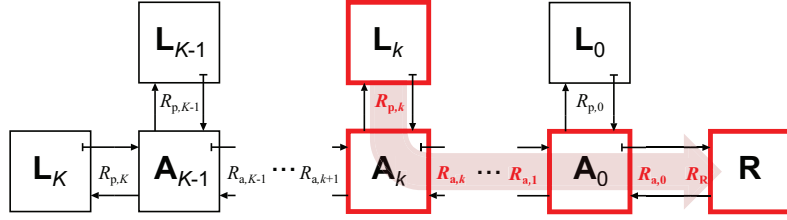


Figure 2.4. Overview of the ports whose impedances need to be updated when the port resistance of element \mathbf{L}_k is changed.

2.4.3 Nonlinear elements

Nonlinear circuit elements may also be defined for WDFs. If a memoryless nonlinearity is considered, it will be defined by an instantaneous current-to-voltage mapping $V = f_e(I)$. Notice that even though memoryless nonlinear elements are considered here, they may have dynamic effects when connected to reactive circuits. The implementation of this mapping may be converted to the wave domain in order to obtain the outgoing wave $B = f_w(A, R_p)$ [54]. In general there is no exact solution for adapting these elements, and they have to be placed at the root of the tree. Thus practical WDF networks may only have one such nonlinear element. The computation of the function $f_w(A, R_p)$ may be realized either by a look-up table or using an analytical expression. As an example of this approach, an ideal diode may be modeled. This component is an open circuit when the input voltage is larger than zero, and a short circuit otherwise. In that case, the outgoing wave can be easily calculated as

$$B = f_w(A, R_p) = |A|, \quad (2.18)$$

which results in $V = A$ and $I = 0$ for $A > 0$, and $V = 0$ and $I = A/R_p$ for $A < 0$. The implementation of a diode using an analytical expression was used in Publication IV and a look-up-table-based triode is implemented in [60].

Another option for implementing nonlinear memoryless elements is a voltage-dependent resistance. This has the advantage of not being required to be placed at the root of the tree if the resistance is calculated

using a voltage measured at a previous sample. This leads to the possibility of implementing networks with multiple nonlinear elements. Multiple nonlinearities are required for modeling some circuits such as the vacuum tube circuits in Publication III and [61, 62]. One disadvantage of this method is the extra impedance update required when the nonlinear element is not the root, as in Fig. 2.4. However, this problem can be managed by placing the nonlinear elements as close to the root as possible, which reduces the number of adaptors to be updated. Additionally, the delay used to calculate the nonlinear resistance prevents the system from satisfying the conservation of numerical energy, which may cause instability in the system [41]. This problem may be handled by oversampling in WDF networks [63, 61]. By using this approach, the ideal diode can be approximated by

$$R = \begin{cases} R_{oc}, & \text{if } V > 0, \\ R_{sc}, & \text{otherwise,} \end{cases} \quad (2.19)$$

where R_{oc} is a large resistance that approximates an open circuit, and R_{sc} is a small resistance that approximates a short-circuit. Notice that zero and infinity resistances cannot be used in linear resistances which are not placed at the root of the WDF network, since they would result in delay-free elements. However, a good approximation is achieved when very large or small resistance values are used.

When multiple nonlinearities are included in a WDF network, these nonlinearities may be combined into a single multiport element [64]. In this case, the instability caused by the delays is avoided, and a more accurate response of the system is obtained. However, this type of solution is not modular, being against the well-known modularity advantages of traditional WDF networks. An example of a wave-digital triode model using this principle is presented in [65], which is based on the Cardarilli model [66].

Nonlinearities with memory typically require other modeling strategies. As an example, a voltage-controlled capacitor may not keep the energy balance of the circuit when its capacitance varies. For this reason, one option for implementing voltage or current-controlled capacitors or inductors is to connect a constant memory element to the network through an ideal transformer with a voltage-controlled turns ratio [67]. This approach is used in Publication III. Another strategy consists of connecting a nonlinear resistor to the network through a mutator [53, 54, 68]. A mutator is an element that transforms resistors into reactive elements.

In both cases, the change in the equivalent impedance does not result in energy variation.

2.4.4 Computational complexity

The computational complexity of WDF networks is analyzed in Publication IV. From Table 2.1 and Fig. 4 of Publication III, the linear elements are seen to require neither multiplication nor addition, but only memory elements and sign inverting blocks. Three-port series and parallel adaptors can be efficiently implemented using one multiplication and four additions [69, 70]. Finally, the complexity of the root element will depend on the type of element being simulated, e.g. a non-adapted linear element or a nonlinear element. Hence, the complexity of WDF networks can be generally said to be $\mathcal{O}(N)$, where N is the number of tree-port adaptors in the network. N will generally be $N = M - 2$, where M is the number of one-port elements.

2.5 Black-box methods

Understanding some systems to be modeled may be very challenging. As an example, a system may be too complex to be modeled using physical models. In this case, it is highly desirable to obtain automatic modeling methods which do not require detailed knowledge about the system, such as black-box models. The black-box models comprise a set of tools in which only the input-output relationship of a system is modeled. Thus, the internal states of a system are ignored in this type of method, as shown in Fig. 2.1.

A Volterra filter is an example of a black-box model, which provides the most complete representation of nonlinear systems [71, 72, 73]. It is usually trained with algorithms that optimize the output error [71, 72, 73], but it can also be obtained by analyzing the system behavior [14]. Volterra filters have been applied to weakly nonlinear audio systems [74, 14, 75], since they are able to represent any type of nonlinear system, and they provide a good technique for audio system modeling. Volterra models can also be inverted using operator based solutions [76]. However, Volterra filters are complex and difficult to train, and there are audio-specific techniques that are better suited to the problems presented in this thesis. Simplification of a Volterra model can be achieved by using a Wiener

model, whose computational complexity can be further reduced by using the Laguerre transformation [77]. Other models include determining a different impulse response of the nonlinear system for each sample of the input [78, 79, 80].

2.5.1 Swept-sine methods

A simplified method to determine the nonlinear response of audio systems is the swept-sine technique [81, 82]. This method was originally developed to measure the impulse response of systems or rooms [83, 81], but it was later extended for auralization of nonlinear systems [82].

The swept-sine method starts by injecting the test signal having an instantaneous frequency given by a logarithmically increasing sweep [84]

$$f_i(t) = f_1 e^{\frac{t}{T_R}}, \quad (2.20)$$

where f_1 is the initial frequency,

$$T_R = \frac{T f_1}{\ln(f_2/f_1)} \quad (2.21)$$

controls the rate of exponential increase, T is the signal length, and f_2 is the maximum frequency. The sweep with an instantaneous frequency given by Eq. 2.20 has a good property for nonlinear system identification, since the instantaneous frequency of a harmonic frequency of $f_i(t)$ is given by a constant time shift, or

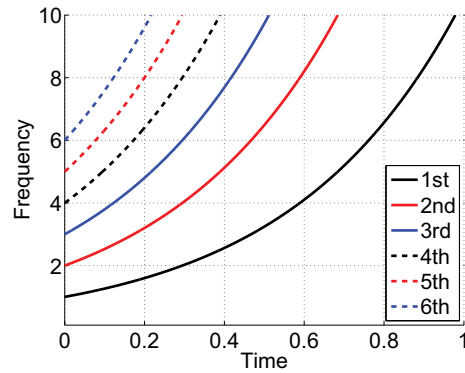
$$f_i(t + \delta t_m) = m f_i(t), \quad (2.22)$$

where

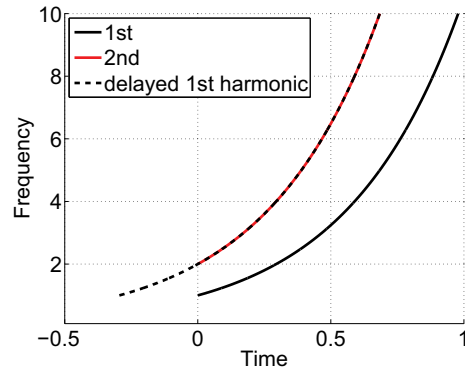
$$\delta t_m = T_R \log(m). \quad (2.23)$$

An example of the swept-sine excitation signal frequency with its harmonics is presented in Fig. 2.5. Figure 2.5 (a) presents the instantaneous frequency of six harmonics while Fig. 2.5 (b) shows that the instantaneous frequency of the second harmonic is a time-shifted version of the instantaneous frequency of the first harmonic, as presented in Eq. 2.22. Figure 2.5 (b) and Eq. 2.22 indicate that, if the output signal of the system is filtered by a signal that inverts the group delay response of the excitation signal, the impulse response of each harmonic will be separated in time at time instants given by Eq. 2.23. This time-domain separation is shown in Fig. 2.5 (c). The inverse filter is either obtained by time-inverting the instantaneous frequency response with energy compensation for the high

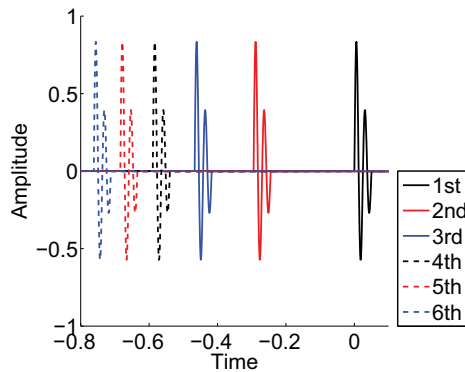
frequencies [81, 82, 85], by an extension of the time-inverted filter that models the full bandwidth of higher order harmonics [86], or by inverting the excitation signal in frequency domain [84, 87].



(a)



(b)



(c)

Figure 2.5. Swept-sine method concept overview. (a) Time-frequency representation of the response of a nonlinear system to a swept sine signal; (b) time-frequency representation of the first and second harmonics of that system; and (c) representation of how the harmonic impulse response is obtained after inverse filtering.

Once the impulse responses of each individual harmonic have been obtained, they may be used either to analyze the nonlinear system or to emulate it. A nonlinear system may be analyzed by visualizing the frequency response of each harmonic, which provides a compact way of characterizing the nonlinear system performance [88]. Publications III and IV as well as [65, 45, 40, 50, 89, 49, 63] use this approach to compare the model results with measurements or reference simulations.

In order to emulate the system with harmonic impulse responses obtained as in Fig. 2.5 (c), the impulse responses are cascaded with polynomial waveshapers, as shown in Fig. 1 of Publication V. The configuration of memoryless nonlinearities followed by linear filters is called the Hammerstein model [90, 86, 73]. The impulse responses of the individual harmonics are mapped onto the equivalent impulse responses of the polynomial waveshapers. Farina [82] defines the formulas for this mapping up to the fifth harmonic in frequency domain, which are generalized by Novák [85] for any harmonic component. Rebillat [87] also presents a time-domain approach for determining the filters using Chebyshev polynomials.

Although the swept-sine method is able to properly model Hammerstein systems, it has two primary disadvantages. The first is that, since the obtained model is a Hammerstein type, it is not generalized for all nonlinear systems, specially when linear filtering is applied before the nonlinearity, as in Wiener nonlinear systems. For this reason, some systems may be better represented by other types of models. In order to resolve this problem, multiple excitation amplitudes in the swept-sine analysis may be applied and the result is used to train a Volterra system [91]. The second problem of modeling with the swept-sine method is its computational complexity. When modeling high-order systems, the model will be implemented with a number of polynomial-waveshapers/filter pairs whose order is as large as the highest harmonic generated by the system. The computational efficiency of these models may be reduced by decomposing the filters into second-order sections and combining the common parts of the different filters [92]. Additionally, a method to combine the waveshaper/filter pairs is proposed in Publication V.

2.6 Discussion

Many modeling techniques are available for audio circuits, and one may be better than another in specific situations. Physical models are well suited to adapting system parameters, since adjusting their values imply only recalculating their coefficients, whereas most of the black-box models would need to be retrained for the new situation. Additionally, physical models are suitable for situations in which performing measurements of the real system is impossible, expensive or dangerous, such as when modeling rare musical equipment, when expensive sensors are needed or when high voltages are involved. On the other hand, black-box models are interesting when there is no information on the circuit schematics, and its input-output relationship can be measured. Moreover, different types of physical modeling techniques can be combined, such as the SS and the WDF [93]. On the other hand, black-box models are particularly suited for systems that are difficult to understand, and its automatic methods may provide a modeling methodology much faster than when using a physical approach.

Among the physical approaches, only the SS and the WDF approaches provide systematic modeling methods, whereas the physically inspired models usually require time-consuming analyses of the system. Although the SS models may be less complex in very specific situations, their asymptotic complexity is generally $\mathcal{O}(N^2)$ due to the matrix multiplications, whereas the WDF's complexity is $\mathcal{O}(N)$. The matrix involved in SS models using nodal analysis are sparse and their solution can be simplified to $\mathcal{O}(N^{1.4})$ [5]. This means that simulation of large circuits will be more efficient when using WDFs than when using SS models.

When nonlinear elements are considered, SS modeling offers more flexibility for accommodating multiple nonlinearities, whereas accurate modeling of WDF allows only for one nonlinear element. However, there are techniques for handling this limitation, such as using multiport elements [64, 65] or using voltage-dependent resistors with delayed resistance values [60, 61]. This approximation may lead to decreased accuracy, which, however, is often not perceived by listeners, specially when oversampling is applied. WDFs also enable modular implementation of the model [32], which enables reuse of code when developing audio software and saves development time when several different systems need to be modeled.

3. Application of circuit modeling of the guitar

This section focuses on circuit modeling applications to guitar equipment. Figure 3.1 shows one example of a guitar setup with some of the circuit elements influencing the timbre of the guitar. In this setup the timbre of the guitar is modified by the pickup response, the cable, the effect boxes, and finally by the amplifier, in addition to the playing techniques. Several different setups may be used by guitar players, including using different types of pickups, effects, and amplifiers, and interchanging effect types. When a digital model of these effects is used, as in Fig. 3.2, many combinations of these models may be chosen, and the user may change its parameters at any time. Hence, it is interesting to have a modular approach to model each of these blocks, since there may be the need for real-time change in the way they are interconnected or in their parameters.

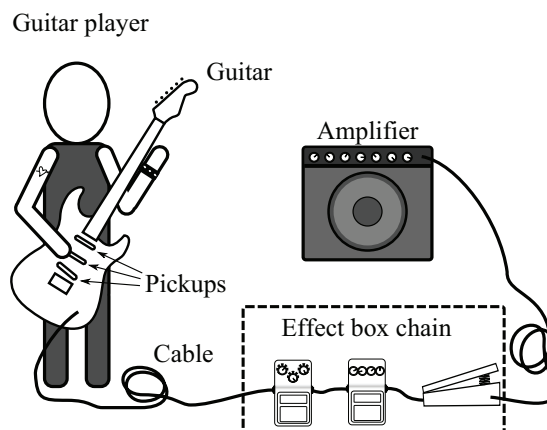


Figure 3.1. Typical guitar setup and audio devices influencing its timbre.

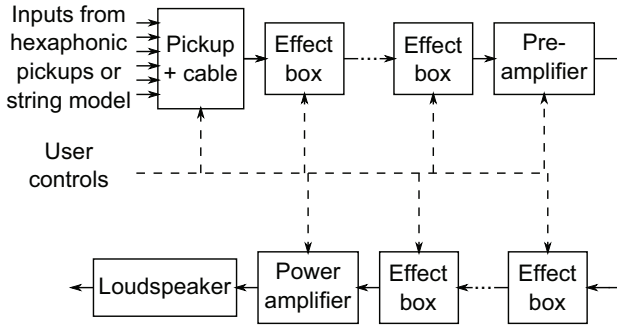


Figure 3.2. Typical setup where digital models are employed.

3.1 Effect box modeling

A significant fraction of guitar effects is implemented as effect boxes. They have the advantage of being portable when compared to guitar amplifiers, and guitar players often include several boxes in their effect chain, as shown in Fig. 3.1.

Many distortion effect boxes employ operational amplifiers and diodes. A general representation of distortion circuits using operational amplifiers is shown in Fig. 3.3(a). In this configuration, the input signal may be fed into the system either at V_{i0} or at V_{i1} while the output is measured at V_{out} . The gain in this circuit is controlled with the impedances Z_0 , Z_1 and Z_f , which combine resistors and capacitors. Additionally, diodes are connected in parallel with the feedback impedance Z_f , which are considered here as a nonlinear impedance R_{NL} . R_{NL} is usually composed of two anti-parallel diodes, but other configurations are also used [49, 89]. Additionally, other circuits may contain operational amplifier stages with a diode clipper between them, as does the Boss DS1 [35].

The diodes comprise an important part in the circuit of Fig. 3.3(a). When operating in the forward-bias region the diodes are conducting. In this region they have small resistance and have a nearly constant voltage drop between its terminals, as shown in Fig. 3.3(b) [94]. Additionally, when a voltage is applied in the reverse-bias region, a small amount of current flows through the diode terminals, which, however, is negligible for the diode-based distortions.

The schematic of Fig. 3.3 allows for two main configurations. The first one is the inverting configuration, where the input signal is applied to V_{i0} and V_{i1} is grounded, resulting in an output signal with inverted polarity. On the other hand, if the input signal is applied to V_{i1} and V_{i0} is grounded,

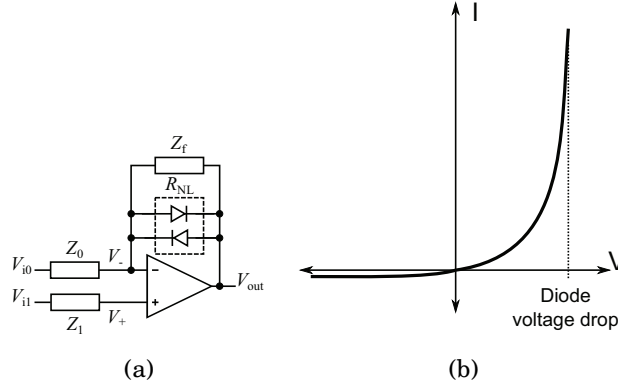


Figure 3.3. Operational amplifier general distortion circuit: (a) a typical operational amplifier configuration and (b) the diode nonlinear voltage-current characteristic curve.

the output has the same polarity as the input, resulting in a non-inverting configuration. If operated in the linear region, the circuit of Fig. 3.3 has a gain [94]

$$G_{\text{inv}} = -\frac{Z_f}{Z_0} \quad (3.1)$$

for the inverting configuration, and

$$G_{\text{noninv}} = 1 + \frac{Z_f}{Z_0} \quad (3.2)$$

for the non-inverting configuration. However, when the output amplitude exceeds the diode drop voltage, a current starts to flow through the diodes, causing the equivalent gain to be

$$\lim_{Z_f \rightarrow 0} G_{\text{inv}} = 0, \quad (3.3)$$

$$\lim_{Z_f \rightarrow 0} G_{\text{noninv}} = 1, \quad (3.4)$$

for the inverting and the non-inverting configurations, respectively.

Equation 3.3 indicates that when an inverting operational amplifier distortion reaches the saturation limit changes in the input will not affect the output. At this stage, the output voltage is kept at a constant value. Figure 3.4(a) shows the input-to-output mapping of the inverting circuit when only memoryless elements are used in Z_f and Z_0 . When the output voltage reaches the diode drop voltage the circuit is seen to saturate. Additionally, this result is illustrated in Fig. 3.5(a) for a sinusoidal input. In this case, the output voltage is a square wave when a high amplifier gain is used, whereas it is smoother for a small gain. Hence, the inverting configuration is used for building hard-clipping distortion circuits.

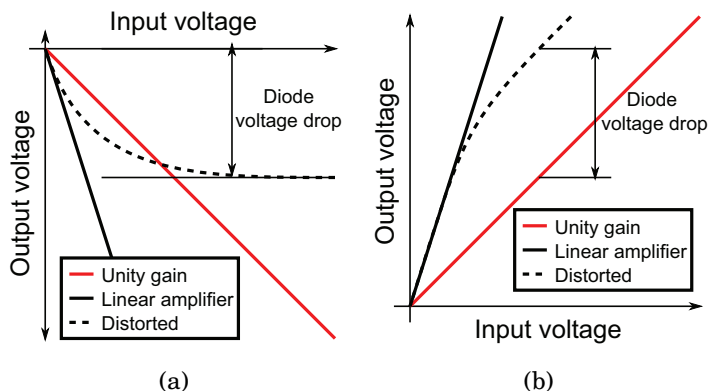


Figure 3.4. Operational amplifier input-output mapping when ignoring memory elements for the (a) inverting and (b) non-inverting configurations.

The non-inverting configuration, on the other hand, has unity gain after reaching saturation, as stated in Eq. 3.4. This suggests that the output voltage continues to increase after the saturation limit of the diode is reached, but with a smaller gain. Figure 3.4(b) shows the memoryless input-output mapping of the non-inverting configuration, where the output increases with a unity-gain slope after saturation is reached. This result is further clarified with an example where a sine wave is fed into the kind of nonlinearity in Fig. 3.5(b), where the output wave after saturation is the same as the input wave, but with a constant shift given by the diode voltage drop. When the polarity of the input signal is changed, the diode in the opposite direction starts to conduct, resulting in a voltage shift with the same polarity as the input voltage.

Several virtual analog papers concentrate on the operational amplifier and diode distortion circuits. Some of them simplify the problem by simulating only the diode, with a resistor and capacitor used as a clipper. An ideal diode WDF model is presented in [93], whereas the diode clipper is approximated by a memoryless static nonlinearity in a physically inspired model in [48]. It was found that this static nonlinearity is not as accurate as solving the system differential equations [34, 35]. A WDF and SS diode model is presented in [48], where the WDF diode model uses numerical methods for determining the diode outgoing wave. A linear time-variant filter is used to model the diode clipper circuit in [95], in which an iterative Newton procedure is used to find the voltage-dependent diode filter coefficients. SS equations with the K method have been used to derive the model of a Marshall JCM900 preamplifier circuit using inverting operational amplifier distortion in [49], whereas a Boss SD1 non-inverting cir-

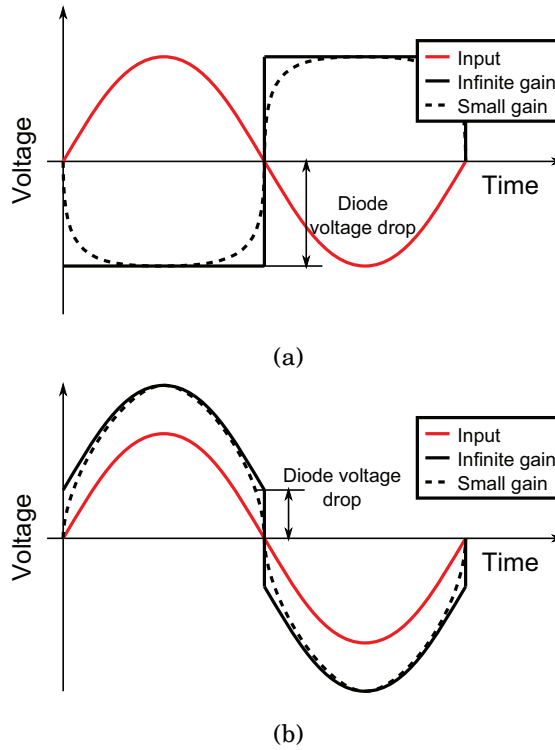


Figure 3.5. Operational amplifier distortion input/output mapping when ignoring memory elements for the (a) inverting and (b) non-inverting configurations.

circuit with tree diodes in the feedback impedance is modeled in [89]. Other effect-box related work include the modeling of a transconductance amplifier using SS representation with the K method [96]. A black-box model of a non-inverting distortion circuit is also presented in [97, 85].

A general problem of SS models is that any update in the circuit elements reflects on the calculation of the matrices. A distortion circuit is modeled using SS equations in [49] and an efficient way to handle the distortion parameter through a matrix representation that avoids inversion when changing this parameter is presented. This problem is important when designing circuits that continuously change their parameters, such as the wah-wah. [50] looks at this issue by decomposing the SS matrix into parts that are independent of the wah-wah potentiometer resistance and uses the Woodbury identity to simplify the matrix inverse calculation. Additionally, the wah-wah model can be obtained through a simplified physically-inspired linear implementation [98] or using the bilinear transform [99, 2], which also has an efficient coefficient update.

Publication IV proposes a new generic model of the circuit of Fig. 3.3(a).

In this model a simplified ideal operational amplifier model is derived, which splits the circuit of Fig. 3.3(a) into subcircuits. These subcircuits are derived so as to eliminate an implicit relationship between them, and one subcircuit output is used as an input to another. Hence, a WDF model without delay-free loops could be derived. Additionally, the diode non-linear function is modeled by a closed-form formula using the Lambert function [100, 101], which avoids the need of interactive methods as in [48].

3.2 Guitar amplifier modeling

Guitar amplifiers play a significant role in the modification of the guitar timbre. Normal audio amplifiers are responsible mostly for amplifying the audio signal and feeding it to one or more loudspeakers, as shown in Fig. 3.6(a). On the other hand, guitar amplifiers often include nonlinear distortion that is considered pleasing for guitars. Figure 3.6(b) shows an example of how the input signal may be distorted in a guitar amplifier. Hence, the guitar amplifier has traditionally served not only as a means of signal amplification, but also as an effect for enhancing the guitar timbre. Additionally, the same holds also for the guitar amplifier loudspeaker, which differs from linear high-fidelity loudspeakers.

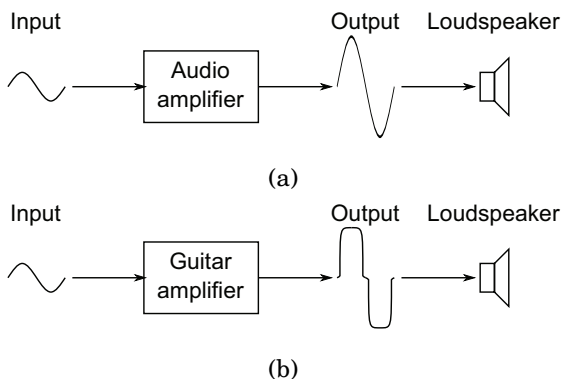


Figure 3.6. Schematic diagram of the difference of (a) general-purpose audio amplifiers and (b) guitar amplifiers.

Most of the traditional guitar amplifiers are built using vacuum tubes. This type of component was popular for building electronic circuits before the invention of silicon-based electronic devices, such as transistors. Hence, by the time the first electric guitars were invented, vacuum tubes were the only option for building guitar amplifiers. Additionally, since

many legendary guitar players became famous using vacuum-tube amplifiers, their timbre is still highly appreciated by musicians, which is claimed to be one of the reasons why vacuum tubes are preferred over transistors for guitar amplification.

However, there are practical problems that make vacuum-tube amplifiers not as practical as modern transistor amplifiers [4]. Firstly, the music industry is one of the only industries using vacuum tubes, which increases significantly the price of this type of device. Secondly, vacuum tubes are big and cumbersome in comparison to transistors. Thirdly, vacuum tubes are fragile and change their timbre with temperature, humidity, and aging, what causes them to be less reliable than transistors. For the above mentioned reasons, obtaining digital counterparts that emulate the timbre of vacuum tubes is highly desirable.

Figure 3.7 illustrates how a triode modifies the guitar timbre. A triode is a vacuum tube device used to amplify electric signals. This type of circuit has an input voltage V_{in} , a power source V_{cc} , and at least one resistor R_s in series with the element in order to limit the current I_p . When the input varies, the equivalent resistance of the electronic device changes, causing a variation in the current I_p which modifies the voltage at the plate terminal V_{pk} . This means that the output voltage of this simplified circuit is bounded by the power source as $0 < V_{pk} < V_{cc}$.

Figure 3.7(b) shows one example of the voltage V_{pk} when using Koren's triode equations with parameters of the triode 12AX7 [102], $R_s = 100k\Omega$, and different values of V_{cc} . If an ideal linear amplifier is considered, the output voltage follows a linear relationship with the input signal. However the output is bounded by the power source voltage V_{cc} . Additionally, in the region where the output voltage is between zero and V_{cc} , the output is not linearly related to the input. The resulting waveform is shown in Fig. 3.7(c) for a sinusoidal signal between -8.5 and 0.5 V. Figure 3.7(c) shows the harsh clipping discontinuity in the output signal when it reaches zero, which does not depend on the power source V_{cc} . Furthermore, the clipping value and shape for large output voltages depends on the power source voltage V_{cc} , where a smoother clipping shape is observable when V_{cc} is large.

Typical vacuum tube amplifiers are built using several stages of amplification circuits. The first stages are meant for buffering the low-energy signal coming from the guitar pickups and for voltage amplification, comprising the pre-amplifier circuit [103]. These are built using triode stages,

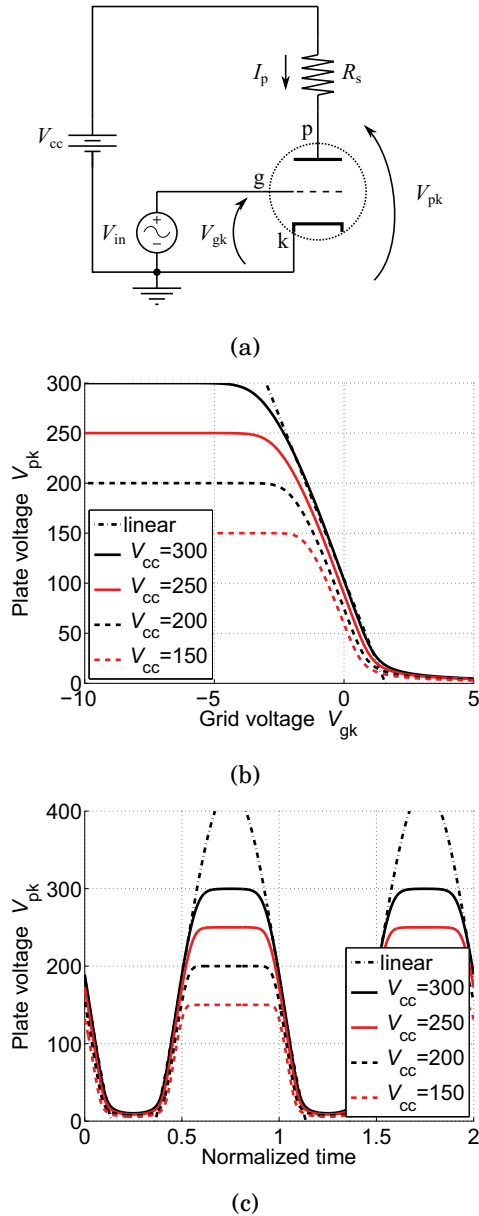


Figure 3.7. Triode nonlinearity example. (a) Simplified triode circuit. (b) Triode plate voltage V_{pk} as a function of the grid voltage V_{gk} for different source voltages. (c) Plate voltage for a sinusoidal grid voltage between -5 and 2.5 volts.

based on the circuit of Fig. 3.7(a), typically including the cathode bias, which enhance the timbre of the guitar with its nonlinearity. In practice, several of these stages may be included in series. Next, a tone control stage is included, which is a simple linear filtering stage where the user is able to control the timbre of the amplifier. The tone-control stage may

be modeled with linear filters obtained with the discretized model of this circuit [37]. Finally, the energy of the signal goes through the power amplifier in order to drive the output loudspeakers. Figure 3.8 shows one example of a power amplifier using a single pentode. This circuit is called single-ended, and other power amplifiers using two pentodes are used in the push-pull configuration that is shown in Fig. 3 of Publication III. In the circuit of Fig. 3.8, an audio transformer is used in order to match the impedance of the loudspeaker and drive it with the correct voltage.

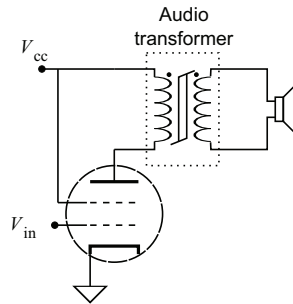


Figure 3.8. Single-ended pentode power amplifier stage example (adapted from [104]).

The power amplifier of Fig. 3.8 includes three sources of nonlinearity. The first is the pentode nonlinearity, which is similar to the triode nonlinearity explained above and illustrated in Fig. 3.7. The second is the audio transformer nonlinearity, which is caused by magnetic saturation and hysteresis. The third is the loudspeaker nonlinearity, which is caused by suspension stiffness, and coil position-dependent induction, among others [105].

The effect of the audio transformer nonlinearity is discussed in Publication III. This nonlinearity cannot be modeled by a static input-output mapping since it happens in the magnetic domain instead of the electric domain. The effect on the output voltage of the nonlinear transformer is shown in Fig. 2 of Publication III. In this example, the output voltage is not clipped as in a memoryless nonlinearity, but it goes to zero after some time when the input voltage is kept at the same polarity, and only begins to increase after the input voltage changes its polarity. Additionally, this nonlinearity is highly dependent on the frequency of the input signal, and low frequencies are more distorted than the high frequencies.

Vacuum-tube mathematical models are fundamental for building amplifier models. Models of vacuum-tube devices based on their physical characteristics using the Child-Langmuir law [106, 107] are shown in [108,

109, 106, 107]. A phenomenological model is presented in [102], with a model that is derived from the behavior of the vacuum tubes, without considering their basic physics. It has been shown that Koren's model [102] fits better to the triode's datasheet information when compared to Leach's model [110, 108]. A polynomial approximation to the measurement data is presented in [111]. An improvement over Koren's phenomenological model including the triode grid current and Miller capacitance is presented in [112, 113], which also includes a fitting procedure for adjusting the model to measured data. A mixed physical-iterpolative model is presented in [66], where the Child-Langmuir equation [106, 107] is taken as the model baseline, and its parameters are adjusted with a polynomial that depends on the grid voltage. A WDF version of this model is developed in [65]. An improvement of Leach's model [108] is developed by modifying the Child-Langmuir equation to use a different exponent coefficient [45]. This model has shown better accuracy when compared to the models in [102, 110]. The model in [45] is extended in [114] in order to include the grid-current dependency on the anode voltage.

The development of triode preamplifiers models is addressed by several works. A physically inspired triode stage is proposed in [115, 116], which uses Koren's triode model [102]. In this model the input signal is processed by a low-pass filter, whose result is the input to a nonlinear function representing the triode behavior. The output of this nonlinear function is fed back to the input using a unit delay, and the resulting signal is processed by a high-pass filter, representing the DC-blocking filter. A triode preamplifier stage model using a numerical solution is presented in [117]. This solution ignores capacitive elements, but the effects of biasing are considered.

A WDF pre-amplifier model is presented in [60]. This model uses a simplified approximation of the triode, and the feedback of the voltage at the cathode is modeled by delaying it and combining to the input voltage. This approximation is enhanced in [61], which models the grid terminal as a diode. In this model, the diode nonlinearity is modeled as a voltage-controlled nonlinear resistance, with the resistance delayed by one sample. This model has advantages when compared to [60], since its approximation of the grid circuit is more precise and emulates properly other effects, such as the blocking distortion [118]. These models are enhanced when applying the WDF polarity inverter [55]. A CSound implementation of the triode stage in [61] is presented in [119].

A pre-amplifier triode model using the SS representation is presented in [110]. This model uses the Runge-Kutta discretization method and Newton's method to solve the implicit nonlinear equation. The authors of the paper verified that increasing the sampling frequency decreases the number of iterations of the algorithm, since the last sample solution is used as an initial estimate, which is close to the solution when the sampling frequency is higher. This model is enhanced by including the parasitic capacitances, the grid rectification effect, and a triode model based on real measurements, which can be used to emulate aging effects [112]. A triode amplifier stage model using the DK method is presented in [44], which also presents results on the required size of the nonlinearity look-up table in order to avoid audible artifacts.

Many papers show that splitting the circuit into sub-circuits decreases the computational complexity for SS methods, with some loss in modeling accuracy [112]. Since the complexity of SS methods is $\mathcal{O}(N^2)$, an approximation of a circuit of size N with M parts of size N/M would theoretically result in a complexity of $\mathcal{O}(N^2/M)$. A preamplifier comprising several triode stages can be approximated in a block-wise manner by simulating blocks of two triode stages [120]. In this method, the first and second triode stages are simulated in a block, and the output of the first triode stage is used as the input to a block containing the second and third triode stages. This arrangement is done in order to consider the nonlinear load that one triode stage presents to the other [121]. This method has reduced the average computational complexity of a SS model of a four-triode stage preamplifier by a factor of between two and four [62]. When WDF simulations are considered, this type of method would not lead to reduced complexity, since WDFs are $\mathcal{O}(N)$. However, this type of method is interesting for dealing with multiple nonlinearities that are not easily handled in WDF.

One important aspect that makes the output stage of a vacuum-tube amplifier different from preamplifier stages is the output transformer. The first attempts to model the output stages of vacuum-tube amplifiers have employed linear models of the transformers. An off-line PSPICE model for analyzing power amplifier topologies is presented in [104]. A linear approximation of the transformer and loudspeaker is also possible by considering both as a simple resistance [120]. However, this model neglects the frequency response of the transformer and its interaction with the circuit. A WDF linear transformer model is presented in [63], which uses

linear circuit elements in order to emulate the transformer's frequency response. A transformer model accounting for leakage inductance and ohmic losses is used in an ODE simulator in [47] and in a WDF simulator in [122].

Electromagnetic transformer models have been widely studied for many years, and the effects caused by magnetic hysteresis are known to the scientific community [123]. General hysteresis models include the Preisach model [124, 125], in which several simple on-off hysteresis nonlinearity are combined in parallel to yield more complex shapes. Optimization of the Preisach model parameters to fit real measurement data is presented in [126, 127]. Another model uses implicit differential equations to represent the magnetic hysteresis [128, 129], and is named Jiles-Atherton after its authors. A method for fitting real data to the Jiles-Atherton model is presented in [130]. However the fitted model is dependent on the characteristics of the input signal, which poses a problem for processing signals with wide dynamic range, such as audio signals. The Jiles-Atherton model has been applied for PSPICE simulations of power amplifiers [131] and for real-time simulation of amplifiers using SS models [132, 133, 46].

Another class of transformer models emerge from the gyrator-capacitor analogy [134, 135]. In this approach, a gyrator is used to map electrical quantities onto magnetic quantities. The gyrator is a circuit element that converts voltages into currents and vice versa. With this transformation, the inductances of the transformer model are turned into capacitances that represent the magnetic flux paths in an intuitive manner. Hence, this technique is particularly useful for modeling multiwinding transformers [136] and integrated magnetics [137]. In this model, a capacitance is used to represent the magnetic permeance of the core. This permeance changes when reaching magnetic saturation, hence it is modeled as a nonlinear capacitance [134]. Additionally, hysteresis is included in the model through a nonlinear resistor [138].

A WDF nonlinear gyrator-capacitor model is developed in Publication III for building a virtual power amplifier. A triode single-ended power amplifier, used as in [63], is modeled utilizing the nonlinear gyrator-capacitor transformer model. This model is extended for the application using WDFs, where a measurement and parameter fitting procedure is proposed to approximate the given transformer.

Another aspect of the output chain of an amplifier is to consider the loudspeaker model. This has been already addressed using a simple low-

pass filter [60] and a linear WDF model [63]. An input-output model of the loudspeaker including a nonlinear function for the voice-coil displacement is presented in [139]. Finally, a black-box model based on the swept-sine analysis is presented in [92].

3.3 Guitar pickup

The electromagnetic pickup comprises the most traditional transducer used to capture the string movement in guitars. Although its primary intent is only to transform string vibration into an electrical signal, it contributes greatly to the guitar timbre. Additionally, other musical instruments, like bass guitars, and the Clavinet, use this type of transducer [16, 17, 18].

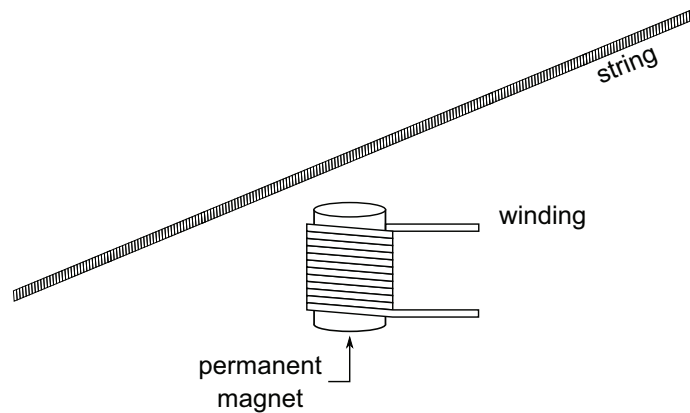


Figure 3.9. Schematic diagram of the pickup building blocks.

The basic construction of a pickup is shown in Fig. 3.9. The pickup is formed of two main parts. The first is a permanent magnet, which has a constant magnetizing force H that creates a magnetic field around it. When the string gets close to the magnet, the permeance μ seen by this magnetizing force decreases, causing an increase in the magnetic flux ϕ around it. The second part is the winding, formed by a wire wound around the permanent magnet, and responsible for translating the variation of the magnetic field to electric signals, since its output voltage E is proportional to the time derivative of the magnetic flux ϕ and the number of turns N as $E = N\dot{\phi}$.

Several types of pickups are commercially available, mainly classified as single-coil and humbucker pickups. Single-coil pickups are those in

which only one magnet and winding is used to capture the vibration of a single string, while humbucker pickups are a combination of two single-coil pickups in close proximity. Humbucker pickups were developed to suppress noise, built using two windings connected so that the induced current flows in opposite directions so as to cancel out the electromagnetic noise captured by the pickups [140]. Additionally, electromagnetic pickups are not the only transducers on the market. There are also piezoelectric and electret-film pickups [141, 142, 143] which are placed on the guitar bridge that convert mechanical tension into an electrical voltage, and hence have very distinct characteristics when compared to the electromagnetic pickups.

One important aspect of electromagnetic pickups, and other non-contact pickups like capacitive or optical, is that their position influences the output timbre, due to the wave propagation properties of strings. This can be understood using a standing-wave methodology [144, 145], as shown in Fig.3 of Publication I. From this figure it is clear that some partials of the string vibration will have nodes close to the pickup position, which indicates that these will be attenuated in comparison to other partials [145, 146]. The different options of pickup combinations also play an important role on the timbre. The phase of mixed pickups is recognized to influence the combined perceived timbre [147], since the phase differences will cause some frequencies to be enhanced or attenuated [148]. Additionally, the sensitivity width of the pickup is also shown to influence its response [145].

Although the standing wave is an intuitive way of understanding the pickup position effect, it fails to provide a model for emulating this effect in audio effects or synthesis systems. For this reason, a digital waveguide (DWG) model of a string can be used to understand this behavior [149, 150, 151]. The DWG comprises a digital solution for the d'Alembert wave equation that describes the movement of a string [152]. This model represents the string movement as the combination of two waves propagating in opposite directions with delay lines representing the time the wave takes to travel between its extremes. This type of model is used to synthesize string and acoustic tube musical instruments [149, 150, 116, 153, 154].

The string motion above the pickup can be derived using the DWG. In this approach, the string motion at a given point is determined as the combination of both waves at that point, from which the pickup transfer

function can be obtained [155]. This transfer function results in a simple comb filter when an ideal string is considered [156, 157, 116], which can be approximated using fractional delay filters [158]. Publication I uses this approach in order to derive a new model for the pickup mixing effect. In this model, two comb filters are applied in series, one representing the average position of the pickups, and the other for the difference between their positions. Additionally, the DWG-based model is used in Publication I to derive the effect the sensitivity width has over the pickup response and to obtain a signal processing model of this effect as a FIR filter whose impulse response has the shape of the sensitivity width function.

However, the ideal string model of the DWG assumes a constant group delay for all frequencies. This is known not to be true in real strings due to dispersion in the string, which causes real strings to be inharmonic [159]. Guitar inharmonicity is mainly perceived in low-pitched strings, which have a higher inharmonicity factor, and can be neglected for high-pitched strings [160]. Modifications of the DWG for synthesis of inharmonic strings have been addressed in several scientific publications by including allpass filters in the feedback loop of the string model, implemented as several first-order allpass sections [161] or a single high-order allpass filter [162, 163, 164]. The allpass sections can also be obtained using first-order allpass sections [165, 166, 167] obtained with frequency-warped signal processing techniques [168, 169, 170, 171]. The same concept that is applied for string synthesis can be used to model the pickup of an inharmonic string [172].

The next effect of the pickup is related to its equivalent circuit. Like any winding around a ferromagnetic core, the pickup has a prominent inductance. Additionally, the close proximity of each winding turn creates a capacitance and the long wire used for the winding creates a resistance. Hence, the pickup can be described by an equivalent resonant circuit containing a resistor, an inductor and a capacitance. This circuit results in a prominent resonant peak whose frequency depends on its physical parameters [173, 174, 146]. Extensive measurements of different pickups have shown that the frequency of this resonance is between 3 kHz and 16 kHz [173]. This equivalent circuit has already been considered for guitar synthesis in [116].

Publication I extends the equivalent circuit analysis in order to obtain a circuit model of pickup mixing. In this model the RLC circuit of the two pickups is analyzed, resulting in two resonances when two pickups

are combined in series and a single resonance otherwise. This model is obtained assuming that both pickups are in the same position. This circuit mixing model is used in combination with the pickup-position mixing model in practice.

The equivalent circuit of the pickup is also used in order to analyze the effect of cables on the guitar timbre. The effect of cables connecting loudspeakers have been analyzed previously [175, 176], and measurements show that the cable interacts with the pickup changing its resonance frequency [173]. Publication II presents the analysis of the effect of the cable when combined with the guitar. In this paper, the impedance of several commercial cables, measured with and without a pickup connected to them, shows a high correlation between the cable capacitance and the pickup resonant frequency.

Finally, the mapping between the string position and the magnetic flux in the pickup is nonlinear. One intuitive manner of understanding this behavior is obtained by analyzing one string vibrating in a direction that is perpendicular to the north-south axis of a permanent magnet. In this case, the maximum magnetic flux will be obtained when the string is directly above the permanent magnet and will decrease if it moves to any side of the magnet. This results in a nonlinearity that maps large positive or negative values of the string position onto a small magnetic flux and a small value onto a large magnetic flux. Hence, a string movement that is parallel to the guitar face is mapped onto a signal with doubled frequency, resulting in even harmonics. This behavior is verified by simulations [177, 178]. On the other hand, if the string moves in the direction of the north-south axis of the permanent magnet, i.e. moving away from the magnet, the magnetic flux gets stronger as the string gets closer to the permanent magnet.

The nonlinear mapping of the magnetic pickup has been modeled using integral equations. In this approach, the permanent magnet is approximated by two cylinders of positive and negative magnetic charge, and the magnetic field at a point in space is determined by calculating the surface integral over these cylinders [177, 178]. As a last step, the string is discretized into finite magnets that cancel the magnetic field caused by the permanent magnet, and their effect is combined in order to obtain the resulting magnetic flux [178]. Publication I presents a 2-D finite-element model that approximates the pickup nonlinear function. This model is simple enough in order to be prepared and simulated offline, and

its results can be used as a look-up-table or with a polynomial approximation [18].

4. Circuit analogies for audio processing and synthesis

Physical analogies provide a useful representation of audio systems, which may be used in two manners. The analogies may be used to transpose the problem equations to another domain, which may be easier for the people involved to understand, or for which there are analysis tools available. Again, the analogies may be used as building blocks for synthesis or effects, as shown in Fig. 4.1. The physical analogies are made here in order to build physically plausible digital systems or to provide physical parameters that are meaningful for a non-technical audience.

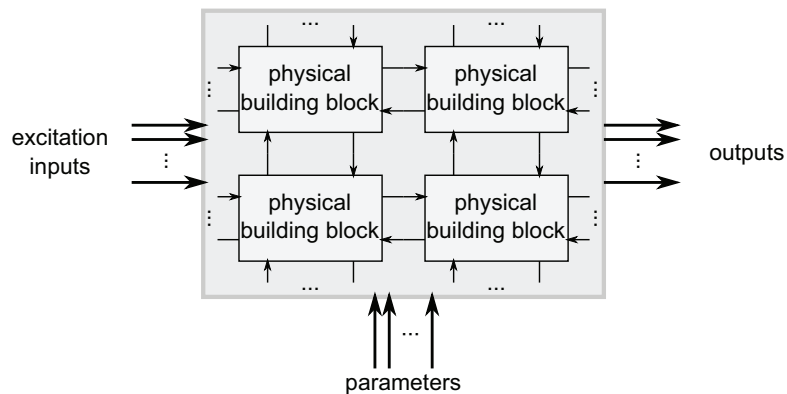


Figure 4.1. Typical synthesis and effect system based on physical analogy blocks.

4.1 Physical analogies

Audio systems use typical analogies between electrical, mechanical, and acoustical domains. Typical equivalent second-order systems are presented in Fig. 4.2, with the corresponding analogous variables presented in Table 4.1 [52, 179]. Other types of analogies are also possible, and yield simpler models of some systems [180]. All the second-order systems of

Fig. 4.2 can be connected with other second-order systems, which results in block-based models of higher-order ODEs.

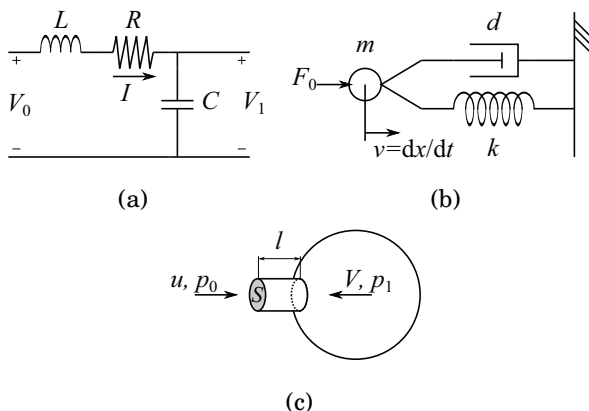


Figure 4.2. Typical second-order lumped systems in the (a) electrical, (b) mechanical, and (c) acoustical domains.

Table 4.1. Common electrical, mechanical, and acoustical analogies, where ρ is the density of air and c is the speed of sound in air in the acoustical domain (adapted from [52]).

Electrical domain	Mechanical domain	Acoustical domain
voltage V	force F	air pressure p
current I	velocity v	volume velocity u
resistance R	viscous damper d	fluid-dynamic resistance $R = \frac{\rho c}{S}$
inductance L	mass m	acoustic inductance of a tube $L = \frac{\rho l}{S}$
capacitance C	inverse spring constant $1/k$	acoustic capacitance of a cavity $C = \frac{V}{\rho c^2}$

Mechanical systems can be compared to electrical circuits, as in Fig. 4.2(a) and (b), since they result in similar differential equations. If the electrical current and voltage are considered as the analog counterparts of the mechanical velocity and force, the mechanical elements are analogous to the electrical elements, as presented in Table 4.1. As a result, mechanical circuits can be readily represented as electrical circuits, and vice versa. One should note, though, that the interconnection type (series or parallel) is not given by the table and may require a bit of thought.

Additionally, acoustic systems can also be represented using analogies. The Helmholtz resonator shown in Fig. 4.2(c) is analogous to the RLC circuit of Fig. 4.2(a) and the mass-spring-damper system of Fig. 4.2(b),

with the analogous physical quantities presented in Table 4.1 [159, 181, 182].

4.2 Applications

Physical analogies have been extensively used in audio synthesis. Mass-spring analogies have been used in systems derived from the CORDIS-ANIMA dynamic simulation engine [31, 183, 184], in which a spring and a damper are represented as digital filters mapping their terminal positions onto forces, and a mass is a digital filter block mapping the forces onto the mass position. In order to resolve delay-free loops contained in the mass-spring network, CORDIS-ANIMA includes a unit delay in the mass block [31, 183].

Mass-spring networks have already been used for composing music [31, 185, 186], in an artificial sand model [187], for building new abstract electronic instruments [188, 189], and modeling musical instruments [190]. Additionally, the inverse sound synthesis using mass-spring networks is described in [191]. The conditions in which the mass-spring network model is stable is discussed in [192]. Mass-spring models were also used to build virtual music instruments that include mechanical feedback [193].

Some musical instruments are also modeled using circuit analogies in order to describe their behavior. The violin string movement is described as a circuit [194], and mass-spring analogies are used to describe the stick-slip behavior of a bowed string [195, 196]. These models are important for understanding the playability limits of bowed string instruments [194, 197].

Circuit analogies have also been used to emulate musical instruments. The piano hammer has a nonlinear behavior, which is modeled as a nonlinear capacitance representing the hammer felt using WDFs [198, 199, 200, 201, 52] and the K method [41]. The tone holes, conical sections, and reed of woodwind instrument bores can be modeled using circuit analogies and emulated with WDFs [202, 203].

Other alternatives for modeling the resonances of a system are also available. The resonances of a system may be modeled as RLC circuit sections and adjusted in order to model the frequency response of a system, such as that in [204]. The modes of a system may be modeled by resonating sections, such as mass-spring sections. These sections are coupled in order to represent the behavior of the system in the coupled-mode

synthesis approach [205]. In the modal synthesis approach, a bank of filters represent the modes of the system, and a matrix is responsible for mapping the excitation signal onto each of these filters [206].

Another approach for modeling physical systems is obtained with the functional transformation method (FTM) [207]. The FTM is used firstly for converting spatially distributed partial differential equations (PDE) to the frequency domain using the Laplace and the Sturm-Liouville transforms, which operate in the time and spatial domains, respectively [208, 209]. As a second step, the frequency domain multidimensional transfer functions are discretized, enabling the simulation of the system [209]. This concept is used to model strings [210, 209, 211], membranes of drums [209, 32], and tubular bells [212]. Additionally, FTM can be combined with WDF, as in the simulation of a membrane excited by a hammer [32].

Acoustic-electric circuit analogies are explored in Publication VI, where the concept of the Helmholtz resonator of Fig. 4.2(c) with its equivalent electric circuit [159, 181, 182] is investigated for building complex systems. In this approach, Helmholtz resonators are connected in a tree-like structure which can be excited at any resonator block.

Most of the techniques described above have the advantage of enabling excitation at different parts of the virtual instrument. This is closely related to the effect of exciting different parts of a percussion instrument in order to explore its timbre variation, such as in the Hang [213]. Different resonators of the Helmholtz resonator tree and different masses of the mass-spring networks can be excited to yield this timbre variation. In the modal synthesis, the excitation mapping matrix can be modified in order to excite the modes differently [206]. The FTM may be used to excite different positions of the system with its initial condition [209]. Additionally, the modularity of these methods enables the combination of several blocks in order to build a complex structure, such as the one in Fig. 4.1.

5. Summary of the main contributions

5.1 Publication I. Acoustics and modeling of pickups

Electromagnetic pickups are important for understanding the timbre of electrical guitars. Publication I introduces a complete analysis on the phenomena that characterize the pickup timbre and introduces new models. New models for the pickup mixing and width effects are derived using a continuous-time traveling wave representation of a string, which are extensions of previous single-pickup single-observation-point models [156, 157, 155]. Additionally, the model of the existing equivalent circuit of the pickup [173] is extended in order to emulate its resonance change when two pickups are combined. Finally, 2-D FEM simulations were used to simulate the pickup nonlinear behavior, which is simpler to implement using existing FEM software in contrast to the existing integral equations describing the pickup [177, 178].

5.2 Publication II. Cable matters: Instrument cables affect the frequency response of electric guitars

Although audio cables are supposed to deliver a signal from one end to another, they have an important effect when used with electric guitars. This work is a natural extension of Publication I, where the effect of combining the impedances of the cable and pickup is analyzed. In this study, the author of this thesis conducted measurements using several commercial cables and a pickup in order to observe this effect. The impedance of the cable was first derived starting from a distributed impedance model, which proved to be equivalent to a simplified lumped impedance model. The measured cables included high quality guitar cables, a long coiled cable,

and an extremely short cable, as shown in Fig. 5.1. Once the impedance of the cables was analyzed, the impedance of the pickup of Fig. 5.2 was measured when combined with the cables. The results show that the cables have a prominent effect on the resonance of the pickup, and that only the capacitance of the cable causes this effect.

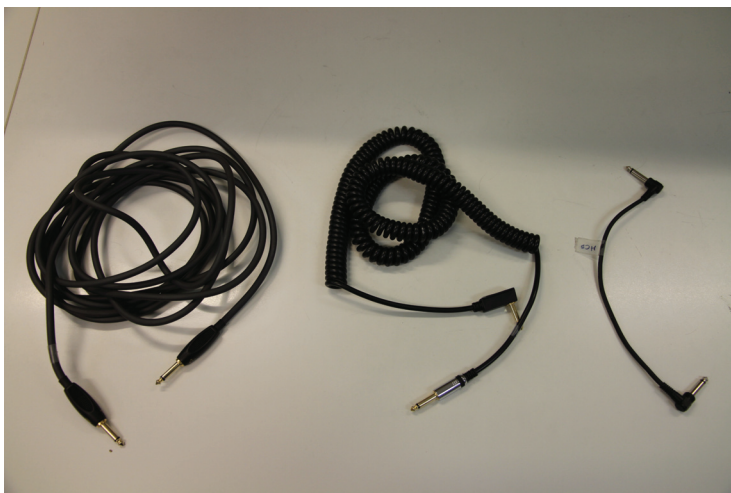


Figure 5.1. Example of cables used in Publication II.



Figure 5.2. Pickup measurement setup used in Publication II.

An informal listening test shows that the cable effect is easily audible. During the poster presentation of this paper, the author of this thesis presented sound samples using two cables to 34 people attending the presentation. The listening environment was noisy and the samples were presented using headphones. In this test, only one listener reported not

to perceive the differences in the cables, while the other 33 listeners reported to perceive a clear difference.

5.3 Publication III. Real-time audio transformer emulation for virtual tube amplifiers

This paper presented the modeling methodology of audio transformers for tube amplifier emulation. The audio transformer is an important part of guitar power amplifiers, since they are required to couple the amplifier to the loudspeaker. Although ideal transformers are supposed to be linear and have a flat frequency response, their nonlinearity may introduce audible effects which are desirable for guitar amplifiers. In this study, the audio transformers shown in Fig. 5.3 were measured. A measurement methodology was developed in order to obtain the parameters for the new proposed transformer model. The results have shown that the Hammond transformer in Fig. 5.3(a) is almost linear in its operation region, while the nonlinearity of the Fender transformer in Fig. 5.3(b) was audible when excited at low frequencies below 100 Hz. Finally, the fitted model was used to simulate a complete WDF model of a single-ended power amplifier including the audio transformer. This transformer model has the advantage of modularity and also enables the simulation of technically challenging conditions, such as when the saturation of the transformer leads to over-heating in a real amplifier.

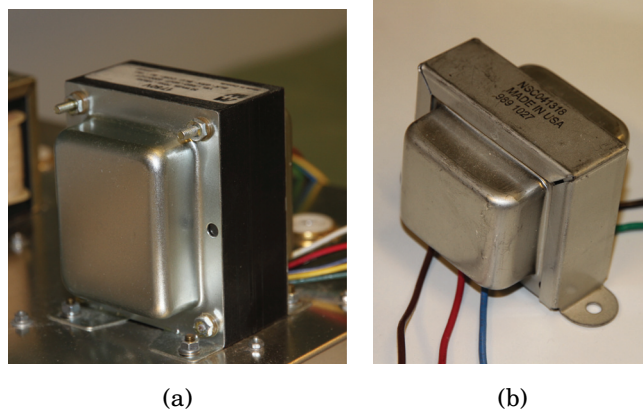


Figure 5.3. Audio transformers measured in Publication III: (a) Hammond T1750V and (b) Fender NSC041318.

Accompanying webpage:

<http://www.acoustics.hut.fi/publications/papers/jasp-trafo/>

5.4 Publication IV. Emulation of operational amplifiers and diodes in audio distortion circuits

This publication presents the development of a new model for modeling distortion circuits based on operational amplifiers and diodes. An operational amplifier model is presented in Publication IV for simulation using WDF. The derivation of the model starts by creating an equivalent circuit of an ideal operational amplifier when connected using negative feedback. This equivalent circuit divides the operational amplifier into three sub-blocks. The first one represents the effect of the input impedance, and the input signal is fed to it. The second represents the amplifier feedback, and it uses the output current of the first circuit as the input. The last one maps the variables of the first and second blocks onto the output. The first block does not depend on the others, while the second block depends only on the first. Hence, the circuit can be calculated in a sequential manner. For this reason, the proposed equivalent circuit is a good candidate for implementation in the wave-digital domain.

The WDF implementation of the operational amplifier circuit follows the ideal equivalent circuit presented previously. Since the circuits do not contain implicit dependencies, the subcircuits can be simulated independently as separate WDF networks. This enables simulation of several operational amplifiers circuits in a straightforward manner.

The WDF operational amplifier model presented in this publication differs from the state-of-the-art since it enables implementation without implicit dependencies. In order to avoid these dependencies, previous WDF-based works included only the diode clipper in the feedback of the circuit [48]. Hence, the approach of Publication IV enables the implementation of the complete operational amplifier-based distortion circuit, where the only simplification assumption made is that the operational amplifier is ideal.

Accompanying webpage: <http://www.acoustics.hut.fi/publications/papers/ieee-cs-2012-opamp/>

5.5 Publication V. Reduced-Complexity Modeling of High-Order Nonlinear Audio Systems Using Swept-Sine and Principal Component Analysis

Black-box models provide a convenient manner for simulating nonlinear audio systems. One of the most popular black-box models is obtained with swept-sine analysis, in which a polynomial Hammerstein model is obtained. Although this model is obtained in a straightforward manner, when high-order systems are modeled, it results in a computationally complex model. The study in Publication V is motivated by this computational problem. This paper uses the principal component analysis (PCA) [214] to reduce the computational complexity of the resulting model. In the proposed approach, the branches of the polynomial Hammerstein model obtained with the swept-sine analysis are combined with the PCA. The final result is a bank of waveshapers and filters pairs. This system is less complex than the traditional swept-sine techniques, since for representing N harmonics of the system it requires N polynomial and filter pairs, while the proposed technique requires a smaller number. The computational cost reduction shown in Publication V is about 66%. Additionally, tests performed in simulated nonlinear systems have shown that 30 harmonics could be represented by two waveshaper and filter pairs, leading to a 93% reduction in the computational cost compared to the original Hammerstein system.

5.6 Publication VI. The Helmholtz resonator tree

This publication presents a new method for building abstract instruments through electro-acoustic analogies. The Helmholtz resonator tree is used to build abstract structures that are intuitive and related to real-world concepts. The resonator tree concept is related to mass-spring networks, although it is built using a different type of analogy. The implementation of the Helmholtz resonator tree concept was based on a WDF C++ tool which was developed by the author of this thesis. In the design phase of this concept, the combination of the resonators in a large structure had to be limited due to the WDF connection restrictions. Hence, the author restricted the connections of the resonators to a tree structure which results in realizable WDF networks. This tool was experimented in different environments, which included a VST plugin running on a computer and

an Android mobile application for running a Helmholtz resonator tree in real-time.

Accompanying webpage: <http://www.acoustics.hut.fi/publications/papers/dafx12-helmholtztree/>

6. Conclusions and directions of future research

This thesis presents circuit modeling techniques and their use in audio. It focuses on two main perspectives. In the first one, circuit modeling techniques are used to simulate existing audio equipment. In the second one, circuit models are used to develop abstract audio synthesis methods, which can be used to build virtual music instruments.

The models of audio equipment developed in this thesis followed physical modeling and black-box approaches. The main method used for physical modeling is based on WDF, since it provides a modular and computationally efficient approach for circuit simulation. Publications III and IV use WDFs to model a transformer and an operational amplifier-based guitar distortion circuit. Other physical modeling techniques, such as the digital waveguide and the bilinear transform are used to obtain models related to electromagnetic pickup phenomena in Publication I, and to understand the effect of the connecting cable on the timbre of guitars in Publication II. The black-box modeling approach is used by enhancing the well known swept-sine techniques. Publication V presents a novel method in which the resulting model from the swept-sine technique has its computational complexity significantly reduced using PCA.

By using circuit modeling techniques, new models were obtained for analog audio equipment. In Publication III, a new nonlinear audio transformer model is used in the real-time emulation of a virtual guitar power amplifier. Until the time of publication of Publication III there were no scientific publications on the real-time emulation of nonlinear audio transformers, but now other publications are available on the topic [133, 46].

In Publication IV a new operational amplifier model was presented to emulate distortion circuits. Although this model was applied using WDFs, it could be readily applied using other techniques, such as SS. The opera-

tional amplifier model has the advantage of decoupling different parts of the circuit, enabling the partitioning of distortion circuits into sub-circuits. Additionally, the pickup was studied in Publication I. In this work, new models for mixed pickups are proposed analyzing both the positions of the pickups and their circuit impedance. Additionally, the model for the pickup width is derived, and finite element simulations were used to demonstrate the pickup nonlinearity. This work was extended in order to describe the effects of the cable-pickup interaction on the timbre of the guitar in Publication II.

Circuit models also have applications in musical synthesis. By using circuit analogies, build damped oscillating structures that create plausible synthetic sounds is possible. Publication VI uses electro-acoustic analogies to build a resonating structure that can be used for synthesis. This structure was built by connecting Helmholtz resonator blocks with each other, resulting in a complex high-order resonating system, whose parameters can be changed in a physically intuitive manner.

This thesis has dealt with several aspects of circuit modeling in audio. Theoretical development with mathematical derivation of models was done in Publications I, IV, and V. Several aspects of the practical implementation of WDF networks were approached: BlockCompiler [215] was used in Publication III, the Simulink tool in Publication IV, and a C++ WDF tool was developed by the author in Publication VI. The models were verified using Matlab in all the publications. Furthermore, practical measurement methodologies were developed for the audio transformer and the pickup-cable integration in Publications II and III. Finally, a practical implementation of a WDF network in C++ was developed for both VST plugins and the Android mobile phone platform in Publication VI.

Future directions on nonlinear circuit modeling could be related to aliasing effects. Alias suppression has already been addressed in oscillators for digital subtractive synthesis in [216, 217, 218]. Nonlinear circuits have used oversampling to avoid this effect, but other new techniques would be highly desirable. Additionally, future guitar distortion circuits could use perceptual descriptors, such as the ones described in [219], in their user interfaces. This could enable building intuitive user interfaces for digital distortion circuits, where users use perceptually relevant parameters to control the resulting timbre.

Errata

Publication I

- Fig. 8 caption should read *Fig. 8. Comb filter implementation for equal pickup mixing for (a) out-of-phase and (b) in-phase configurations.*

Publication III

- Fig. 9(d) has an error on the y-axis scale. It should be from -40 to 60 dB as in Fig. 9(c).

Publication VI

- Equation (3) should read $C = \frac{V_0}{\rho c^2}$.
- The variable for the length of the neck in Section 2.3, 5.2, and 5.3 is L when it should be l .
- The variable for the area of the neck in Section 5.3 is A when it should be S .

Bibliography

- [1] V. Välimäki, F. Fontana, J. O. Smith, and U. Zölzer, “Introduction to the special issue on virtual analog audio effects and musical instruments,” *IEEE Trans. Audio, Speech, and Language Processing*, vol. 18, no. 4, pp. 713–714, May 2010.
- [2] V. Välimäki, S. Bilbao, J. O. Smith, J. Abel, J. Pakarinen, and D. Berners, “Virtual analog effects,” in *DAFX - Digital Audio Effects*, U. Zölzer, Ed., chapter 12, pp. 473–522. John Wiley & Sons, 2nd edition, 2011.
- [3] J. Pakarinen, V. Välimäki, F. Fontana, V. Lazzarini, and J. S. Abel, “Recent advances in real-time musical effects, synthesis, and virtual analog models,” *EURASIP J. Advances Signal Processing*, vol. 2011, pp. 1–15, 2011.
- [4] E. Barbour, “The cool sound of tubes [vacuum tube musical applications],” *IEEE Spectrum*, vol. 35, no. 8, pp. 24–35, Aug. 1998.
- [5] J. Pakarinen and D. T. Yeh, “A review of digital techniques for modeling vacuum-tube guitar amplifiers,” *Computer Music J.*, vol. 33, no. 2, pp. 85–100, 2009.
- [6] V. Välimäki and A. Huovilainen, “Oscillator and filter algorithms for virtual analog synthesis,” *Computer Music J.*, vol. 30, no. 2, pp. 19–31, 2006.
- [7] V. Lazzarini and J. Timoney, “New perspectives on distortion synthesis for virtual analog oscillators,” *Computer Music J.*, vol. 34, no. 1, pp. 28–40, 2010.
- [8] J. Pekonen, V. Lazzarini, J. Timoney, and V. Välimäki, “Discrete-time modelling of the Moog sawtooth oscillator waveform,” *EURASIP J. Advances Signal Processing*, vol. 2011, pp. 1–15, 2011.
- [9] S. Tassart, “Band-limited impulse train generation using sampled infinite impulse responses of analog filters,” *IEEE Trans. Audio, Speech, and Language Processing*, vol. 21, no. 3, pp. 488–497, March 2013.
- [10] T. Stilson and J. O. Smith, “Analyzing the Moog VCF with considerations for digital implementation,” in *Proc. ICMC’96, Int. Computer Music Conf.*, Hong Kong, 1996, pp. 398–401.
- [11] A. Huovilainen, “Non-linear digital implementation of the Moog ladder filter,” in *Proc. DAFx’04, 7th Int. Conf. Digital Audio Effects*, Naples, Italy, Oct. 2004, pp. 61–64.

- [12] F. Fontana, “Preserving the structure of the Moog VCF in the digital domain,” in *Proc. ICMC’07, Int. Computer Music Conf.*, Copenhagen, Denmark, Aug. 2007, pp. 27–31.
- [13] M. Civolani and F. Fontana, “A nonlinear digital model of the EMS VCS3 voltage-controlled filter,” in *Proc. DAFx’08, 11th Int. Conf. Digital Audio Effects*, Espoo, Finland, Sep. 2008, pp. 35–42.
- [14] T. Hélie, “Volterra series and state transformation for real-time simulations of audio circuits including saturations: Application to the Moog ladder filter,” *IEEE Trans. Audio, Speech, and Language Processing*, vol. 18, no. 4, pp. 747–759, May 2010.
- [15] S. Zambon and F. Fontana, “Efficient polynomial implementation of the EMS VCS3 filter,” in *Proc. DAFx’11, 14th Int. Conf. Digital Audio Effects*, Paris, France, Sep. 2011, pp. 287–290.
- [16] S. Bilbao and M. Rath, “Time domain emulation of the Clavinet,” in *Proc. 128th Audio Engineering Society Conv.*, London, UK, May 2010, Preprint 8014.
- [17] L. Gabrielli, V. Välimäki, and S. Bilbao, “Real-time emulation of the Clavinet,” in *Proc. ICMC’11, Int. Computer Music Conf.*, Huddersfield, UK, Aug. 2011, pp. 249–252.
- [18] L. Remaggi, L. Gabrielli, R. Cauduro Dias de Paiva, V. Välimäki, and S. Squartini, “A pickup model for the Clavinet,” in *Proc. DAFx’12, 15th Int. Conf. Digital Audio Effects*, York, UK, Sep. 2012, pp. 79–83.
- [19] R. Hoffmann-Burchardi, “Digital simulation of the diode ring modulator for musical applications,” in *Proc. DAFx’08, 11th Int. Conf. Digital Audio Effects*, Espoo, Finland, Sep. 2008, pp. 165–168.
- [20] J. Parker, “A simple digital model of the diode-based ring-modulator,” in *Proc. DAFx’11, 14th Int. Conf. Digital Audio Effects*, Paris, France, Sep. 2011, pp. 163–166.
- [21] C. Raffel and J. O. Smith, “Practical modeling of bucket-brigade device circuits,” in *Proc. DAFx’08, 11th Int. Conf. Digital Audio Effects*, Espoo, Finland, Sep. 2008, pp. 50–56.
- [22] S. Bilbao and J. Parker, “A virtual model of spring reverberation,” *IEEE Trans. Audio, Speech, and Language Processing*, vol. 18, no. 4, pp. 799–808, May 2010.
- [23] J. Parker, “Efficient dispersion generation structures for spring reverb emulation,” *EURASIP J. Advances Signal Processing*, vol. 2011, pp. 18, 2011.
- [24] E. K. Pritchard, “Semiconductor amplifier with tube amplifier characteristics,” US Patent 4809336, Feb. 1989.
- [25] B. Keir, “Solid state audio amplifier emulating a tube audio amplifier,” US Patent 5467400, Nov. 1995, Assignee: Marshall Amplification Plc.
- [26] M. Doidic, M. Mecca, M. Ryle, and C. Senffner, “Tube modeling programmable digital guitar amplification system,” US Patent 5789689, Aug. 1998.

- [27] M. N. Gallo, "Method and apparatus for distortion of audio signals and emulation of vacuum tube amplifiers," 2008, U.S. Patent Application 2008/0218259 A1. Filed Mar. 6, 2007, published Sep. 11, 2008.
- [28] C. Kemper, "Musical instrument with acoustic transducer," US Patent 20080134867 A1, Jun. 2008.
- [29] S. Gelineck and S. Serafin, "A practical approach towards an exploratory framework for physical modeling," *Computer Music J.*, vol. 34, no. 34, pp. 51–65, 2010.
- [30] A. Fettweis, "Wave digital filters: Theory and practice," *Proc. of the IEEE*, vol. 74, no. 2, pp. 270–327, Feb. 1986.
- [31] C. Cadoz, A. Luciani, and J. L. Florens, "CORDIS-ANIMA: A modeling and simulation system for sound and image synthesis: The general formalism," *Computer Music J.*, vol. 17, no. 1, pp. 19–29, 1993.
- [32] R. Rabenstein, S. Petrausch, A. Sarti, G. De Sanctis, C. Erkut, and M. Karjalainen, "Block-based physical modeling for digital sound synthesis," *IEEE Signal Processing Magazine*, vol. 24, no. 2, pp. 42–54, Mar. 2007.
- [33] R. A. Gallien and K. A. Robertson, "Programmable tone control filters for electric guitar," 2008, U.S. Patent Application 2007/0168063 A1. Filed Jan. 18, 2006, published Jul. 19, 2007.
- [34] D. Yeh, J. Abel, and J. Smith, "Simulation of the diode limiter in guitar distortion circuits by numerical solution of ordinary differential equations," in *Proc. DAFx'07, 10th Int. Conf. Digital Audio Effects*, Bordeaux, France, Sep. 2007, pp. 197–204.
- [35] D. T. Yeh, J. S. Abel, A. Vladimirescu, and J. O. Smith, "Numerical methods for simulation of guitar distortion circuits," *Computer Music J.*, vol. 32, no. 2, pp. 23–42, 2008.
- [36] R. Boylestad, *Introductory Circuit Analysis*, Pearson - Prentice Hall, Upper Saddle River, N.J., 12th edition, 2010.
- [37] D. Yeh and J. O. Smith, "Discretization of the '59 Fender Bassman tone stack," in *Proc. DAFx'06, 9th Int. Conf. Digital Audio Effects*, Montreal, Canada, Sep. 2006, pp. 1–6.
- [38] D. Yeh, J. Abel, and J. Smith, "Simplified, physically-informed models of distortion and overdrive guitar effects pedals," in *Proc. DAFx'07, 10th Int. Conf. Digital Audio Effects*, Bordeaux, France, Sep. 2007, pp. 189–196.
- [39] D. Yeh, J. Nolting, and J. O. Smith, "Physical and behavioral circuit modeling of the SP-12 sampler," in *Proc. ICMC'07, Int. Computer Music Conf.*, Copenhagen, Denmark, Aug. 2007, pp. 26–31.
- [40] S. Oksanen and V. Välimäki, "Modeling of the carbon microphone nonlinearity for vintage telephone sound effect," in *Proc. DAFx'11, 14th Int. Conf. Digital Audio Effects*, Paris, France, Sep. 2011, pp. 27–30.
- [41] G. Borin, G. De Poli, and D. Rocchesso, "Elimination of delay-free loops in discrete-time models of nonlinear acoustic systems," *IEEE Trans. Speech and Audio Processing*, vol. 8, no. 5, pp. 597–605, Sep. 2000.

- [42] D. T. Yeh, J. S. Abel, and J. O. Smith, "Automated physical modeling of nonlinear audio circuits for real-time audio effects – part I: Theoretical development," *IEEE Trans. Audio, Speech, and Language Processing*, vol. 18, no. 4, pp. 728–737, May 2010.
- [43] A. Antoniou and W.-S. Lu, *Practical Optimization: Algorithms and Engineering Applications*, Springer, 2007.
- [44] D. T. Yeh, "Automated physical modeling of nonlinear audio circuits for real-time audio effects – part II: BJT and Vacuum Tube examples," *IEEE Trans. Audio, Speech, and Language Processing*, vol. 20, no. 4, pp. 1207–1216, May 2012.
- [45] K. Dempwolf and U. Zölzer, "A physically-motivated triode model for circuit simulations," in *Proc. DAFx'11, 14th Int. Conf. Digital Audio Effects*, Paris, France, Sep. 2011, pp. 257–264.
- [46] J. Mačák, "Nonlinear transformer simulation for real-time digital audio signal processing," in *Proc. TSP'12, 34th Int. Conf. Telecommunications and Signal Processing*, 2012.
- [47] I. Cohen and T. Hélie, "Real-time simulation of a guitar power amplifier," in *Proc. DAFx'10, 13th Int. Conf. Digital Audio Effects*, Graz, Austria, Sep. 2010, pp. 30–33.
- [48] D. T. Yeh and J. O. Smith, "Simulating guitar distortion circuits using wave digital and nonlinear state-space formulations," in *Proc. DAFx'08, 11th Int. Conf. Digital Audio Effects*, Espoo, Finland, Sep. 2008, pp. 19–26.
- [49] K. Dempwolf, M. Holters, and U. Zölzer, "Discretization of parametric analog circuits for real-time simulations," in *Proc. DAFx'10, 13th Int. Conf. Digital Audio Effects*, Graz, Austria, Sep. 2010, pp. 42–49.
- [50] M. Holters and U. Zölzer, "Physical modeling of a Wah-Wah effect pedal as a case study for application of the nodal DK method to circuits with variable parts," in *Proc. DAFx'11, 14th Int. Conf. Digital Audio Effects*, Paris, France, Sep. 2011, pp. 31–35.
- [51] S. Bilbao, *Wave and Scattering Methods for Numerical Simulation*, John Wiley and Sons, 2004.
- [52] V. Välimäki, J. Pakarinen, C. Erku, and M. Karjalainen, "Discrete-time modelling of musical instruments," *Reports on Progress in Physics*, vol. 69, no. 1, pp. 1–78, Jan. 2006.
- [53] A. Sarti and G. De Poli, "Generalized adaptors with memory for nonlinear wave digital structures," in *Proc. EUSIPCO'96, 8th European Signal Processing Conf.*, Trieste, Italy, 1996, pp. 1773–1776.
- [54] A. Sarti and G. De Poli, "Toward nonlinear wave digital filters," *IEEE Trans. Signal Processing*, vol. 47, no. 6, pp. 1654–1688, Jun. 1999.
- [55] S. D'Angelo and V. Välimäki, "Wave-digital polarity and current inverters and their application to virtual analog audio processing," in *Proc. ICASSP'12, IEEE Int. Conf. Acoustics, Speech and Signal Processing*, Kyoto, Japan, Mar. 2012, pp. 469–472.

- [56] G. De Sanctis, A. Sarti, and S. Tubaro, "Automatic synthesis strategies for object-based dynamical physical models in musical acoustics," in *Proc. DAFx'03, 14th Int. Conf. Digital Audio Effects*, London, England, Sep. 2003, pp. 219–224.
- [57] A. Sarti and G. De Sanctis, "Systematic methods for the implementation of nonlinear wave-digital structures," *IEEE Trans. Circuits and Systems I: Regular Papers*, vol. 56, no. 2, pp. 460–472, Feb. 2009.
- [58] D. Fränken, J. Ochs, and K. Ochs, "Generation of wave digital structures for networks containing multiport elements," *IEEE Trans. Circuits and Systems I: Regular Papers*, vol. 52, no. 3, pp. 586–596, Mar. 2005.
- [59] G. De Sanctis and A. Sarti, "Virtual analog modeling in the wave-digital domain," *IEEE Trans. Audio, Speech, and Language Processing*, vol. 18, no. 4, pp. 715–727, May 2010.
- [60] M. Karjalainen and J. Pakarinen, "Wave digital simulation of a vacuum-tube amplifier," in *Proc. ICASSP'06, IEEE Int. Conf. Acoustics, Speech, and Signal Processing*, Toulouse, France, May 2006, pp. 153–156.
- [61] J. Pakarinen and M. Karjalainen, "Enhanced wave digital triode model for real-time tube amplifier emulation," *IEEE Trans. Audio, Speech, and Language Processing*, vol. 18, no. 4, pp. 738–746, 2010.
- [62] J. Mačák and J. Schimmel, "Real-time guitar preamp simulation using modified blockwise method and approximations," *EURASIP J. Advances Signal Processing*, vol. 2011, pp. 1–11, 2011.
- [63] J. Pakarinen, M. Tikander, and M. Karjalainen, "Wave digital modeling of the output chain of a vacuum-tube amplifier," in *Proc. DAFx'09, 12th Int. Conf. Digital Audio Effects*, Como, Italy, Sep. 2009, pp. 55–59.
- [64] S. Petrausch and R. Rabenstein, "Wave digital filters with multiple nonlinearities," in *Proc. EUSIPCO'04, 12th European Signal Processing Conf.*, Vienna, Austria, Sep. 2004, pp. 77–80.
- [65] S. D'Angelo, J. Pakarinen, and V. Välimäki, "New family of wave-digital triode models," *IEEE Trans. Audio, Speech, and Language Processing*, vol. 21, no. 2, pp. 313–321, Feb. 2013.
- [66] G. Cardarilli, M. Re, and L. Di Carlo, "Improved large-signal model for vacuum triodes," in *IEEE Intl. Symp. Circuits and Systems (ISCAS)*, Taipei, Taiwan, May 2009, pp. 3006–3009.
- [67] M. Karjalainen, "BlockCompiler documentation," 2008, Unfinished report, available on-line at <http://www.acoustics.hut.fi/software/BlockCompiler/docu.html>.
- [68] A. Sarti and G. De Sanctis, "Memory extraction from dynamic scattering junctions in wave digital structures," *IEEE Signal Processing Letters*, vol. 13, no. 12, pp. 729–732, Dec. 2006.
- [69] A. Fettweis and K. Meerkotter, "On adaptors for wave digital filters," *IEEE Trans. Acoustics, Speech, and Signal Processing*, vol. 23, no. 6, pp. 516–525, Dec. 1975.

- [70] M. Karjalainen, "Efficient realization of wave digital components for physical modeling and sound synthesis," *IEEE Trans. Audio, Speech, and Language Processing*, vol. 16, no. 5, pp. 947–956, Jul. 2008.
- [71] P. S. R. Diniz, *Adaptive Filtering: Algorithms and Practical Implementations*, Kluwer, 2nd edition, 2002.
- [72] T. Ogunfunmi, *Adaptive Nonlinear System Identification: The Volterra and Wiener Model Approaches*, Springer Series in Signals and Communication Technology, 2007.
- [73] F. Giri and E.-W. Bai, *Block-oriented Nonlinear System Identification*, Springer, 2010.
- [74] T. Hélie, "On the use of Volterra series for real-time simulation of weakly nonlinear audio devices: application to the Moog ladder filter," in *Proc. DAFx'06, 9th Int. Conf. Digital Audio Effects*, Montreal, Canada, Sep. 2006, pp. 7–12.
- [75] T. Hélie, "Lyapunov stability analysis of the Moog ladder filter and dissipativity aspects in numerical solutions," in *Proc. DAFx'11, 14th Int. Conf. Digital Audio Effects*, Paris, France, Sep. 2011, pp. 45–52.
- [76] A. Sarti and S. Pupolin, "Recursive techniques for the synthesis of a p^{th} -order inverse of a Volterra system," *European Trans. on Telecommunications*, vol. 3, no. 4, pp. 315–322, Jul. 1992.
- [77] J. Schattschneider and U. Zölzer, "Discrete-time models for non-linear audio systems," in *Proc. DAFx'99, 2nd Int. Conf. Digital Audio Effects*, Trondheim, Norway, Dec. 1999, pp. 45–48.
- [78] M. J. Kemp, "Analysis and simulation of non-linear audio processes using finite impulse responses derived at multiple impulse amplitudes," in *Proc. 106th Audio Engineering Society Conv.*, Munich, Germany, May 1999, Preprint 4919.
- [79] M. J. Kemp, "Audio effects synthesizer with or without analyzer," US Patent 7039194, Aug. 1997.
- [80] J. Kemp and H. Primack, "Impulse response measurement of nonlinear systems: Properties of existing techniques and wide noise sequences," *J. Audio Engineering Society*, vol. 59, no. 12, pp. 953–963, Dec. 2011.
- [81] A. Farina, "Simultaneous measurement of impulse response and distortion with a swept-sine technique," in *Proc. 108th Audio Engineering Society Conv.*, Paris, France, Feb. 2000, Preprint 5093.
- [82] A. Farina, "Non-linear convolution: A new approach for the auralization of distorting systems," in *Proc. 110th Audio Engineering Society Conv.*, Amsterdam, The Netherlands, May 2001, Preprint 5359.
- [83] M. A. Poletti, "Linearly swept frequency measurements, time-delay spectrometry, and the wigner distribution," *J. Audio Engineering Society*, vol. 36, no. 6, pp. 457–468, Jun. 1988.
- [84] A. Novák, L. Simon, F. Kadlec, and P. Lotton, "Nonlinear system identification using exponential swept-sine signal," *IEEE Trans. Instrumentation and Measurement*, vol. 59, no. 8, pp. 2220–2229, 2010.

- [85] A. Novák, L. Simon, and P. Lotton, “Analysis, synthesis, and classification of nonlinear systems using synchronized swept-sine method for audio effects,” *EURASIP J. Advances Signal Processing*, vol. 2010, pp. 8, 2010.
- [86] A. Novák, *Identification of Nonlinear Systems in Acoustics*, PhD thesis, Universite du Maine, Le Mans, France, 2009.
- [87] M. Rébillat, R. Hennequin, E. Corteel, and B. F. G. Katz, “Identification of cascade of Hammerstein models for the description of nonlinearities in vibrating devices,” *J. Sound and Vibration*, vol. 330, no. 5, pp. 1018–1038, Feb. 2011.
- [88] J. Pakarinen, “Distortion analysis toolkit - a software tool for easy analysis of nonlinear audio systems,” *EURASIP J. Advances Signal Processing*, vol. 2010, pp. 1–13, 2010.
- [89] M. Holters, K. Dempwolf, and U. Zölzer, “A digital emulation of the Boss SD-1 super overdrive pedal based on physical modeling,” in *Proc. 131st Audio Engineering Society Conv.*, New York, USA, Oct. 2011, Preprint 8506.
- [90] A. Hammerstein, “Nichtlineare Integralgleichungen nebst Anwendungen,” *Acta Mathematica*, vol. 54, no. 1, pp. 117–176, Jul. 1930.
- [91] J. S. Abel and D. P. Berners, “A technique for nonlinear system measurement,” in *Proc. 121th Audio Engineering Society Conv.*, San Francisco, USA, Oct. 2006, Preprint 6951.
- [92] B. Bank, “Computationally efficient nonlinear Chebyshev models using common-pole parallel filters with the application to loudspeaker modeling,” in *Proc. 130th Audio Engineering Society Conv.*, London, UK, May 2011, Preprint 8416.
- [93] S. Petrausch and R. Rabenstein, “Interconnection of state space structures and wave digital filters,” *IEEE Trans. Circuits and Systems II: Express Briefs*, vol. 52, no. 2, pp. 90–93, Feb. 2005.
- [94] R. Boylestad and L. Nashelsky, *Electronic Devices and Circuit Theory*, Prentice Hall, 8th edition, 2002.
- [95] J. Mačák and J. Schimmel, “Nonlinear circuit simulation using time-variant filter,” in *Proc. DAFx’09, 12th Int. Conf. Digital Audio Effects*, Como, Italy, Sep. 2009, pp. 85–89.
- [96] O. Kröning, K. Dempwolf, and U. Zölzer, “Analysis and simulation of an analog guitar compressor,” in *Proc. DAFx’11, 14th Int. Conf. Digital Audio Effects*, Paris, France, Sep. 2011, pp. 205–208.
- [97] A. Novák, L. Simon, P. Lotton, and J. Gilbert, “Chebyshev model and synchronized swept sine method in nonlinear audio effect modeling,” in *Proc. DAFx’10, 13th Int. Conf. Digital Audio Effects*, Graz, Austria, Sep. 2010, pp. 423–427.
- [98] P. Dutilleul, M. Holters, S. Disch, and U. Zölzer, “Filters and delays,” in *DAFX - Digital Audio Effects*, U. Zölzer, Ed., chapter 2, pp. 47–82. John Wiley & Sons, 2nd edition, 2011.

- [99] J. O. Smith, "Virtual electric guitars and effects using Faust and Octave," in *Proc. LAC'08, 6th Int. Linux Audio Conf.*, Toronto, Canada, Feb. 2008, pp. 1–10.
- [100] A. Ortiz-Conde, F. J. García Sánchez, and J. Muci, "Exact analytical solutions of the forward non-ideal diode equation with series and shunt parasitic resistances," *SolidState Electronics*, vol. 44, no. 10, pp. 1861–1864, Oct. 2000.
- [101] D. Veberic, "Having fun with Lambert W(x) function," *CoRR*, vol. abs/1003.1628, 2010.
- [102] N. Koren, "Improved vacuum-tube models for SPICE simulations," *Glass Audio*, vol. 8, pp. 18–27, 1996.
- [103] P. Dutilleux, K. Dempwolf, M. Holters, and U. Zölzer, "Nonlinear processing," in *DAFX - Digital Audio Effects*, U. Zölzer, Ed., chapter 4, pp. 101–138. John Wiley & Sons, 2nd edition, 2011.
- [104] M. Veen and P. Touzelet, "New vacuum tube and output transformer models applied to the Quad II valve amplifier," in *Proc. 114th Audio Engineering Society Conv.*, Amsterdam, Netherlands, Mar. 2003, Preprint 5748.
- [105] W. Klippel, "Loudspeaker nonlinearities - causes, parameters, symptoms," in *Proc. 119th Audio Engineering Society Conv.*, New York, USA, Oct. 2006, Preprint 6584.
- [106] I. Langmuir, "The effect of space charge and residual gases on thermionic currents in high vacuum," *Phys. Rev.*, vol. 2, pp. 450–486, Dec. 1913.
- [107] C. D. Child, "Discharge from hot cao," *Phys. Rev. (Series I)*, vol. 32, pp. 492–511, May 1911.
- [108] W. M. Leach, Jr., "SPICE models for vacuum-tube amplifiers," *J. Audio Engineering Society*, vol. 43, no. 3, pp. 117–126, Mar. 1995.
- [109] C. Rydel, "Simulation of electron tubes with SPICE," in *Proc. 98th Audio Engineering Society Conv.*, Paris, France, Feb. 1995, Preprint 3965.
- [110] I. Cohen and T. Hélie, "Simulation of a guitar amplifier stage for several triode models: examination of some relevant phenomena and choice of adapted numerical schemes," in *Proc. 127th Audio Engineering Society Conv.*, New York, USA, Oct. 2009, Preprint 7929.
- [111] N. Koren, "A generalized algebraic technique for modeling triodes," *Glass Audio*, vol. 10, pp. 2–9, 1998.
- [112] I. Cohen and T. Hélie, "Measures and parameter estimation of triodes, for the real-time simulation of a multi-stage guitar preamplifier," in *Proc. 129th Audio Engineering Society Conv.*, San Francisco, USA, Nov. 2010, Preprint 8219.
- [113] I. Cohen and T. Hélie, "Measures and models of real triodes, for the simulation of guitar amplifiers," in *Proc. Acoustics Conf.*, Nantes, France, Apr. 2012.

- [114] K. Dempwolf, M. Holters, and U. Zölzer, “A triode model for guitar amplifier simulation with individual parameter fitting,” in *Proc. 131st Audio Engineering Society Conv.*, New York, USA, Oct. 2011, pp. 257–264, Preprint 8507.
- [115] M. Karjalainen, T. Mäki-Patola, A. Kanerva, A. Huovilainen, and P. Jänis, “Virtual air guitar,” in *Proc. 117th Audio Engineering Society Conv.*, San Francisco, USA, Oct. 2004, Preprint 6203.
- [116] M. Karjalainen, T. Mäki-Patola, A. Kanerva, and A. Huovilainen, “Virtual air guitar,” *J. Audio Engineering Society*, vol. 54, no. 10, pp. 964–980, Oct. 2006.
- [117] F. Santagata, A. Sarti, and S. Tubaro, “Non-linear digital implementation of a parametric analog tube ground cathode amplifier,” in *Proc. DAFx’07, 10th Int. Conf. Digital Audio Effects*, Bordeaux, France, Sep. 2007, pp. 169–172.
- [118] R. Aiken, “What is blocking distortion?,” 2006, <http://www.aikenamps.com/BlockingDistortion.html> (visited in Jan. 19, 2012).
- [119] M. Fink and R. Rabenstein, “A Csound opcode for a triode stage of a vacuum tube amplifier,” in *Proc. DAFx’11, 14th Int. Conf. Digital Audio Effects*, Paris, France, Sep. 2011, pp. 365–370.
- [120] J. Mačák and J. Schimmel, “Real-time guitar tube amplifier simulation using an approximation of differential equations,” in *Proc. DAFx’10, 13th Int. Conf. Digital Audio Effects*, Graz, Austria, Sep. 2010, pp. 43–41.
- [121] J. Mačák, “Verification of blockwise method for simulation of guitar amplifiers on a guitar tube preamp,” *Elektrorevue*, vol. 1, no. 2, pp. 16–21, Jun. 2010.
- [122] P. Raffensperger, “A wave digital filter model of the Fairchild 670 limiter,” in *Proc. DAFx’12, 15th Int. Conf. Digital Audio Effects*, York, UK, Sep. 2012, pp. 195–202.
- [123] E. Della Torre, *Magnetic Hysteresis*, Wiley-IEEE Press, 1st edition, 1999.
- [124] F. Preisach, “Über die magnetische Nachwirkung,” *Zeitschrift für Physik*, vol. 94, no. 5-6, pp. 277–302, 1935.
- [125] A. Pokrovskii, “Systems with hysteresis,” <http://euclid.ucc.ie/hysteresis/> (visited in Feb. 13, 2013).
- [126] Y. Bernard, E. Mendes, and F. Bouillault, “Dynamic hysteresis modeling based on Preisach model,” *IEEE Trans. Magnetics*, vol. 38, no. 2, pp. 885–888, Mar. 2002.
- [127] E. Fallah and J.S. Moghani, “A new identification and implementation procedure for the isotropic vector Preisach model,” *IEEE Trans. Magnetics*, vol. 44, no. 1, pp. 37–42, Jan. 2008.
- [128] D. C. Jiles and D. L. Atherton, “Theory of ferromagnetic hysteresis (invited),” *J. Applied Physics*, vol. 55, no. 6, pp. 2115–2120, Mar. 1984.

- [129] D. C. Jiles and D. L. Atherton, "Theory of ferromagnetic hysteresis," *J. Magnetism and Magnetic materials*, vol. 61, no. 1-2, pp. 48–60, Sep. 1986.
- [130] J. H. Chan, A. Vladimirescu, X.-C. Gao, P. Liebmann, and J. Valainis, "Non-linear transformer model for circuit simulation," *IEEE Trans. Computer-Aided Design of Integrated Circuits and Systems*, vol. 10, no. 4, pp. 476–482, Apr. 1991.
- [131] P. Touzelet, "Accurate non linear models of valve amplifiers including output transformers," in *Proc. 120th Audio Engineering Society Conv.*, Paris, France, May 2006, Preprint 6830.
- [132] J. Mačák and J. Schimmel, "Simulation of a vacuum-tube push-pull guitar power amplifier," in *Proc. DAFx'11, 14th Int. Conf. Digital Audio Effects*, Paris, France, Sep. 2011, pp. 59–62.
- [133] J. Mačák, "Nonlinear audio transformer simulation using approximation of differential equations," *Elektrorevue*, vol. 2, no. 4, pp. 22–29, Dec. 2011.
- [134] D.C. Hamill, "Gyrator-capacitor modeling: a better way of understanding magnetic components," in *Proc. APEC'94, 9th Applied Power Electronics Conf. and Exposition*, Feb. 1994, pp. 326–332 vol.1.
- [135] R. Buntentbach, "A generalized circuit model for multiwinding inductive devices," *IEEE Trans. Magnetics*, vol. 6, no. 1, pp. 65, Mar. 1970.
- [136] D. C. Hamill, "Lumped equivalent circuits of magnetic components: the gyrator-capacitor approach," *IEEE Trans. Power Electronics*, vol. 8, no. 2, pp. 97–103, Apr. 1993.
- [137] Y.-S. Lee, L.-P. Wong, and D.K.-W. Cheng, "Simulation and design of integrated magnetics for power converters," *IEEE Trans. Magnetics*, vol. 39, no. 2, pp. 1008–1018, Mar. 2003.
- [138] Q. Chen, L. Xu, X. Ruan, S. C. Wong, and C.K. Tse, "Gyrator-capacitor simulation model of nonlinear magnetic core," in *Proc. APEC'09, 24th Annual IEEE Applied Power Electronics Conf. and Exposition*, Feb. 2009, pp. 1740–1746.
- [139] D. T. Yeh, B. Bank, and M. Karjalainen, "Nonlinear modeling of a guitar loudspeaker cabinet," in *Proc. DAFx'08, 11th Int. Conf. Digital Audio Effects*, Espoo, Finland, Sep. 2008, pp. 89–96.
- [140] T. D. Rossing, R. F. Moore, and P. A. Wheeler, *The Science of Sound*, Addison-Wesley, 3rd edition, 2002.
- [141] M. Karjalainen, V. Välimäki, H. Raisanen, and H. Saastamoinen, "DSP equalization of electret film pickup for acoustic guitar," in *Proc. 106th Audio Engineering Society Conv.*, Munich, Germany, May 1999, Preprint 4907.
- [142] M. Karjalainen, V. Välimäki, H. Penttinen, and H. Saastamoinen, "DSP equalization of electret film pickup for the acoustic guitar," *J. Audio Engineering Society*, vol. 48, no. 12, pp. 1183–1193, Dec. 2000.

- [143] H. Penttinen and M. Tikander, “Sound quality differences between electret film (EMFIT) and piezoelectric under-saddle guitar pickups,” in *Proc. 120th Audio Engineering Society Conv.*, Paris, France, May 2006, Preprint 6669.
- [144] T. D. Rossing and G. Caldersmith, “Guitars and lutes,” in *The Science of String Instruments*, T. D. Rossing, Ed., chapter 3, pp. 19–46. Springer, 1st edition, 2010.
- [145] J. D. Tillman, “Response effects of guitar pickup position and width,” Oct. 2002, <http://www.till.com/articles/PickupResponse/index.html> (visited in Mar. 10, 2013).
- [146] C. Gough, “Electric guitar and violin,” in *The Science of String Instruments*, T. D. Rossing, Ed., chapter 22, pp. 393–415. Springer, 1st edition, 2010.
- [147] D. J. Dailey, *Electronics for Guitarists*, Springer, 2011.
- [148] J. D. Tillman, “Response effects of guitar pickup mixing,” Jul. 2000, <http://www.till.com/articles/PickupResponse/index.html> (visited in Dec. 10, 2010).
- [149] J. O. Smith, “Physical modeling using digital waveguides,” *Computer Music J.*, vol. 16, no. 4, pp. 74–91, 1992.
- [150] V. Välimäki, J. Huopaniemi, M. Karjalainen, and Z. Jánosy, “Physical modeling of plucked string instruments with application to real-time sound synthesis,” *J. Audio Engineering Society*, vol. 44, no. 5, pp. 331–353, May 1996.
- [151] P. Cook, “Computer music,” in *Springer Handbook of Acoustics*, T. D. Rossing, Ed., chapter 17, pp. 713–742. Springer, 2001.
- [152] N. Lee and J. O. Smith, “Virtual string synthesis,” in *The Science of String Instruments*, T. D. Rossing, Ed., chapter 23, pp. 417–455. Springer, 1st edition, 2010.
- [153] G. Evangelista and F. Eckerholm, “Player–instrument interaction models for digital waveguide synthesis of guitar: Touch and collisions,” *IEEE Trans. Audio, Speech, and Language Processing*, vol. 18, no. 4, pp. 822–832, May 2010.
- [154] S.-J. Cho, U.-P. Chong, and S.-B. Cho, “Synthesis of the Dan Trahn based on a parameter extraction system,” *J. Audio Engineering Society*, vol. 58, no. 6, pp. 498–507, Jun. 2010.
- [155] M. Karjalainen, V. Välimäki, and T. Tolonen, “Plucked-string models: From the Karplus-Strong algorithm to digital waveguides and beyond,” *Computer Music J.*, vol. 2, no. 3, pp. 17–32, 1998.
- [156] C. R. Sullivan, “Extending the Karplus-Strong algorithm to synthesize electric guitar timbres with distortion and feedback,” *Computer Music J.*, vol. 14, no. 3, pp. 26–37, 1990.
- [157] M. Karjalainen, V. Välimäki, and Z. Jánosy, “Towards high-quality sound synthesis of the guitar and string instruments,” in *Proc. ICMC’93, Int. Computer Music Conf.*, Tokyo, Japan, Sep. 1993, pp. 56–63.

- [158] T. I. Laakso, V. Välimäki, M. Karjalainen, and U. K. Laine, "Splitting the unit delay - tools for fractional delay filter design," *IEEE Signal Processing Magazine*, vol. 13, no. 1, pp. 30 – 60, Jan. 1996.
- [159] N. H. Fletcher and T. D. Rossing, *The Physics of Musical Instruments*, Springer-Verlag, 1998.
- [160] H. Järveläinen and M. Karjalainen, "Perceptibility of inharmonicity in the acoustic guitar," *Acta Acustica united with Acustica*, vol. 92, no. 5, pp. 842–847, Oct. 2006.
- [161] J. S. Abel and J. O. Smith, "Robust design of very high-order allpass dispersion filters," in *Proc. DAFX'06, 9th Int. Conf. Digital Audio Effects*, Montreal, Canada, Sep. 2006, pp. 13–18.
- [162] J. Rauhala and V. Välimäki, "Tunable dispersion filter design for piano synthesis," *IEEE Signal Processing Letters*, vol. 13, no. 5, pp. 253 – 256, May 2006.
- [163] J. Rauhala, *Physics-Based Parametric Synthesis of Inharmonic Piano Tones*, Ph.D. thesis, Helsinki University of Technology, Espoo, Finland, 2007.
- [164] J. S. Abel, V. Välimäki, and J. O. Smith, "Robust, efficient design of all-pass filters for dispersive string sound synthesis," *IEEE Signal Processing Letters*, vol. 17, no. 4, pp. 406–409, Apr. 2010.
- [165] S. A. Van Duyne and J. O. Smith, "A simplified approach to modeling dispersion caused by stiffness in strings and plates," in *Proc. ICMC'94, Int. Computer Music Conf.*, Denmark, Sep. 1994, vol. 1, pp. 407–410.
- [166] I. Testa, G. Evangelista, and S. Cavaliere, "Physically inspired models for the synthesis of stiff strings with dispersive waveguides," *EURASIP J. Applied Signal Processing*, vol. 2004, no. 7, pp. 964–977, 2004.
- [167] J. Pakarinen, M. Karjalainen, V. Välimäki, and S. Bilbao, "Energy behavior in time-varying fractional delay filters for physical modeling synthesis of musical instruments," in *Proc. ICASSP'05, IEEE Int. Conf. Acoustics, Speech, and Signal Processing*, Philadelphia, USA, Mar. 2005, vol. 3, pp. 1–4.
- [168] A. Härmä, M. Karjalainen, L. Savioja, V. Välimäki, U. K. Laine, and J. Huopaniemi, "Frequency-warped signal processing for audio applications," *J. Audio Engineering Society*, vol. 48, no. 11, pp. 1011–1031, 2000.
- [169] A. Härmä, *Frequency-Warped Autoregressive Modeling and Filtering*, Ph.D. thesis, Helsinki University of Technology, Espoo, Finland, 2001.
- [170] V. Välimäki, J. S. Abel, and J. O. Smith, "Spectral delay filters," *J. Audio Engineering Society*, vol. 57, no. 7/8, pp. 521–531, 2009.
- [171] G. Evangelista, "Time and frequency-warping musical signals," in *DAFX - Digital Audio Effects*, U. Zölzer, Ed., chapter 11, pp. 447–471. John Wiley & Sons, 2nd edition, 2011.
- [172] N. Lindroos, H. Penttinen, and V. Välimäki, "Parametric electric guitar synthesis," *Computer Music J.*, vol. 35, no. 3, pp. 18–27, Sep. 2011.

- [173] T. Jungmann, “Theoretical and practical studies on the behavior of electric guitar pickups,” M.S. thesis, Department of Electrical Engineering, Acoustics Laboratory, Helsinki University of Technology, Espoo, Finland, 1994.
- [174] M. Koch, *Building Electric Guitars*, Koch Verlag, Nürtingen, Germany, 2001.
- [175] F. E. Davis, “Effects of cable, loudspeaker, and amplifier interactions,” *J. Audio Engineering Society*, vol. 39, no. 6, pp. 461–468, Jun. 1991.
- [176] R. Black, “Audio cable distortion is not a myth,” in *Proc. 120th Audio Engineering Society Conv.*, Paris, France, May 2006, Preprint 6858.
- [177] G. Lemarquand and V. Lemarquand, “Calculation method of permanent-magnet pickups for electric guitars,” *IEEE Trans. Magnetics*, vol. 43, no. 9, pp. 3573–3578, Sep. 2007.
- [178] N. G. Horton and T. R. Moore, “Modeling the magnetic pickup of an electric guitar,” *American J. Physics*, vol. 77, no. 2, pp. 144–150, Feb. 2009.
- [179] V. Välimäki, “Physics-based modeling of musical instruments,” *Acta Acustica united with Acustica*, vol. 90, no. 4, pp. 611–617, Jul. 2004.
- [180] I.J. Busch-Vishniac, *Electromechanical Sensors and Actuators*, Springer Verlag, 1999.
- [181] T. D. Rossing and N. H. Fletcher, *Principles of Vibration and Sound*, Springer-Verlag, 2004.
- [182] A. D. Pierce, “Basic linear acoustics,” in *Springer Handbook of Acoustics*, T. D. Rossing, Ed., chapter 3, pp. 25 – 111. Springer, 2007.
- [183] A. Kontogeorgakopoulos and C. Cadoz, “CORDIS ANIMA physical modeling and simulation system analysis,” in *Proc. SMC’07, 4th Sound and Music Computing Conf.*, Greece, Jul. 2007, pp. 275–282.
- [184] N. Castagné and C. Cadoz, “GENESIS a friendly musician-oriented environment for mass-interaction physical modeling,” in *Proc. ICMC’02, Int. Computer Music Conf.*, Gothenburg, Sweden, 2002, pp. 330–337.
- [185] C. Chafe, “Case studies of physical models in music composition,” in *Proc. ICA’04, 18th Int. Conf. Acoustics*, Kyoto, Japan, Apr. 2004, pp. 2505–2508.
- [186] O. M. Tache and C. Cadoz, “Organizing mass-interaction physical models: the Cordis-Anima musical instrumentarium,” in *Proc. ICMC’09, Int. Computer Music Conf.*, Montreal, Canada, Aug. 2009, pp. 411–414.
- [187] A. Luciani, N. Castagné, and N. Tixier, “Metabolic emergent auditory effects by means of physical particle modeling: the example of musical sand,” in *Proc. DAFx’03, 14th Int. Conf. Digital Audio Effects*, London, UK, Sep. 2003, pp. 63–64.
- [188] J. Kojs, S. Serafin, and C. Chafe, “Cyberinstruments via physical modeling synthesis: Compositional applications,” *Leonardo Music J.*, vol. 17, pp. 61–66, 2007.

- [189] J. Pigott and A. Kontogeorgakopoulos, "Physical thinking: two approaches to mechanical sound design," in *Proc. ICMC'11, Int. Computer Music Conf.*, Huddersfield, UK, Aug. 2011, pp. 253–256.
- [190] A. Kontogeorgakopoulos, P. Tzevelekos, C. Cadoz, and G. Kouroupetroglou, "Using the CORDIS-ANIMA formalism for the physical modeling of the greek Zournas Shawn," in *Proc. ICMC'08, Int. Computer Music Conf.*, Belfast, Northern Ireland, Aug. 2008, pp. 395–398.
- [191] J. M. Villeneuve and C. Cadoz, "Inverse problem in sound synthesis and musical creation using mass-interaction networks," *J. Acoustical Society America*, vol. 4, pp. 2507–2507, 2011.
- [192] D. Morgan and S. Qiao, "Analysis of damped mass-spring systems for sound synthesis," *EURASIP J. Audio, Speech and Music Processing*, vol. 2009, no. 3, pp. 1–19, Jun. 2009.
- [193] E. Berdahl, C. Cadoz, and N. Castagné, "Force-feedback interaction with a neural oscillator model: for shared human-robot control of a virtual percussion instrument," *EURASIP J. Audio, Speech and Music Processing*, vol. 2012, no. 9, pp. 1–14, Feb. 2012.
- [194] J. C. Schelleng, "The bowed string and the player," *J. Acoustical Society of America*, vol. 53, no. 1, pp. 26–41, 1973.
- [195] L. Cremer, *The Physics of the Violin*, The MIT Press, 1983.
- [196] N. H. Fletcher, "The nonlinear physics of musical instruments," *Reports on Progress in Physics*, vol. 62, no. 1, pp. 723–764, May 1999.
- [197] J. Woodhouse, "On the playability of violins. Part 1: Reflection functions," *Acustica*, vol. 78, pp. 125–136, 1993.
- [198] S. A. Van Duyne, J. R. Pierce, and J. O. Smith, "Traveling wave implementation of a lossless mode-coupling filter and the wave digital hammer," in *Proc. ICMC'94, Int. Computer Music Conf.*, Denmark, Sep. 1994, pp. 411–418.
- [199] F. Pedersini, A. Sarti, S. Tubaro, and R. Zattoni, "Toward the automatic synthesis of nonlinear wave digital models for musical acoustics," in *Proc. EUSIPCO'98, 9th European Signal Processing Conf.*, Rhodes, Greece, 1998, pp. 2361–2364.
- [200] F. Pedersini, A. Sarti, and S. Tubaro, "Block-wise physical model synthesis for musical acoustics," *Electronics Letters*, vol. 35, no. 17, pp. 1418–1419, Aug. 1999.
- [201] J. Bensa, S. Bilbao, R. Kronland-Martinet, and J. O. Smith, "A power-normalized non-linear lossy piano hammer," in *Proc. SMAC'03, Stockholm Music Acoustics Conf.*, Stockholm, Sweden, Aug. 2003, pp. 365–368.
- [202] M. van Walstijn and M. Campbell, "Discrete-time modeling of woodwind instrument bores using wave variables," *J. Acoustical Society America*, vol. 113, no. 1, pp. 575–585, Jan. 2003.
- [203] S. Bilbao, J. Bensa, and R. Kronland-Martinet, "The wave digital reed: A passive formulation," in *Proc. DAFx'03, 14th Int. Conf. Digital Audio Effects*, London, England, Sep. 2003, pp. 225–230.

- [204] M. Karjalainen, J. Pakarinen, C. Erkut, P. A. A. Esquef, and V. Välimäki, “Recent advances in physical modeling with K- and W- techniques,” in *Proc. DAFX’04, 7th Int. Conf. Digital Audio Effects04*, Naples, Italy, Oct. 2004, pp. 107–112.
- [205] S. A. Van Duyne, “Coupled mode synthesis,” in *Proc. ICMC’97, Int. Computer Music Conf.*, Thessaloniki, Greece, Sep. 1997, pp. 248–251.
- [206] J. D. Morrison and J. Adrien, “MOSAIC: A framework for modal synthesis,” *Computer Music J.*, vol. 17, no. 1, pp. 45–56, 1993.
- [207] L. Trautmann and R. Rabenstein, *Digital Sound Synthesis by Physical Modeling Using the Functional Transformation Method*, Springer, 2003.
- [208] R. Rabenstein and L. Trautmann, “Multidimensional transfer function models,” *IEEE Trans. Circuits and Systems I: Fundamental Theory and Applications*, vol. 49, pp. 852–861, 2002.
- [209] R. Rabenstein and L. Trautmann, “Digital sound synthesis of string instruments with the functional transformation method,” *Signal Processing*, vol. 83, no. 8, pp. 1673–1688, Aug. 2003.
- [210] L. Trautmann and R. Rabenstein, “Digital sound synthesis based on transfer function models,” in *Proc. IEEE Workshop on Applications of Signal Processing to Audio and Acoustics*, New York, US, Oct. 1999, pp. 83–86.
- [211] L. Trautmann and R. Rabenstein, “Multirate simulations of string vibrations including nonlinear fret-string interactions using the functional transformation method,” *EURASIP J. Applied Signal Processing*, vol. 2004, no. 7, pp. 949–963, Jun. 2004.
- [212] R. Rabenstein, T. Koch, and C. Popp, “Tubular bells: A physical and algorithmic model,” *IEEE Trans. Audio, Speech, and Language Processing*, vol. 18, no. 4, pp. 881–890, May 2010.
- [213] A. B. Morrison and T. D. Rossing, “The extraordinary sound of the hang,” *Physics Today*, vol. 62, no. 3, pp. 66–67, Mar. 2009.
- [214] I. T. Jolliffe, *Principal Component Analysis*, Springer Series in Statistics, 2nd edition, 2002.
- [215] M. Karjalainen, “BlockCompiler: Efficient simulation of acoustic and audio systems,” in *Proc. 114th Audio Engineering Society Conv.*, Amsterdam, Netherlands, Mar. 2003, Preprint 5756.
- [216] H.-M. Lehtonen, J. Pekonen, and V. Välimäki, “Audibility of aliasing distortion in sawtooth signals and its implications for oscillator algorithm design,” *J. Acoustical Society America*, vol. 132, no. 4, pp. 2721–2733, Oct. 2012.
- [217] J. Kleimola and V. Välimäki, “Reducing aliasing from synthetic audio signals using polynomial transition regions,” *IEEE Signal Processing Letters*, vol. 19, no. 2, pp. 67–70, Feb. 2012.
- [218] V. Välimäki, J. Nam, J. O. Smith, and J. S. Abel, “Alias-suppressed oscillators based on differentiated polynomial waveforms,” *IEEE Trans. Audio, Speech, and Language Processing*, vol. 18, no. 4, pp. 786–798, May 2010.

- [219] W. L. Martens and A. Marui, "Multidimensional perceptual scaling of tone color variation in three modeled guitar amplifiers," in *Proc. 112th Audio Engineering Society Conv.*, Munich, Germany, May 2002, Preprint 5552.

Errata

Publication I

- Fig. 8 caption should read *Fig. 8. Comb filter implementation for equal pickup mixing for (a) out-of-phase and (b) in-phase configurations.*

Publication III

- Fig. 9(d) has an error on the y-axis scale. It should be from -40 to 60 dB as in Fig. 9(c).

Publication VI

- Equation (3) should read $C = \frac{V_0}{\rho c^2}$.
- The variable for the length of the neck in Section 2.3, 5.2, and 5.3 is L when it should be l .
- The variable for the area of the neck in Section 5.3 is A when it should be S .



ISBN 978-952-60-5387-5
ISBN 978-952-60-5388-2 (pdf)
ISSN-L 1799-4934
ISSN 1799-4934
ISSN 1799-4942 (pdf)

Aalto University
School of Electrical Engineering
Department of Signal Processing and Acoustics
www.aalto.fi

**BUSINESS +
ECONOMY**

**ART +
DESIGN +
ARCHITECTURE**

**SCIENCE +
TECHNOLOGY**

CROSSOVER

**DOCTORAL
DISSERTATIONS**